Taylor & Francis
Taylor & Francis Group

International Journal of Architectural Heritage

Climate change impact on natural ventilation cooling effectiveness using CFD simulations in low thermal mass historic buildings

Submission ID	245879350
Article Type	Research Article
Keywords	Natural ventilation, Historic buildings, Computational Fluid Dynamics, Building preservation, Future weather
Authors	Layla Iskandar, Carlos Faubel, Ezgi Bay Sahin, Antonio Martinez-Molina, Saadet Toker Beeson

Climate change impact on natural ventilation cooling effectiveness using CFD simulations in low thermal mass historic buildings

Layla Iskandar[a], Carlos Faubel[b*], Ezgi Bay-Sahin[c], Antonio Martinez-Molina[b,d], Saadet Toker Beeson[a]

[a] *School of Architecture and Planning, Klesse College of Engineering and Integrated Design, The University of Texas at San Antonio UTSA, 501 W. César E. Chávez Blvd, San Antonio, TX 78207, USA.*

[b] *Department of Architecture, Design & Urbanism, Antoinette Westphal College of Media Arts and Design, Drexel University, 3501 Market St., Philadelphia, PA 19104, USA.*

[c] *Lancaster School of Architecture, Imagination Lancaster, Lancaster University, Lancaster, UK.*

[d] *Department of Civil, Architectural & Environmental Engineering, College of Engineering, Drexel University, 3141 Chesnut St., Philadelphia, PA 19104, USA.*

*Corresponding Author, e-mail address: cf889@drexel.edu

Abstract

Extreme climate events and global warming significantly affect energy retrofit planning, underscoring the need to consider future climate scenarios. This study evaluates the effectiveness of natural ventilation as a passive cooling strategy for a low-thermal mass building in a hot-humid climate, considering current and future weather conditions throughout this century. Using energy and Computational Fluid Dynamics simulations validated with in-situ data, the research evaluates three natural ventilation strategies: full, cross, and stack ventilation. Results demonstrate that natural ventilation reduces indoor air temperature compared to non-ventilated scenarios but faces challenges in maintaining indoor comfort levels during extreme external temperatures, and under future climate scenarios. Full ventilation is most effective during cooler periods, while cross ventilation significantly enhances airflow across spaces. Stack ventilation shows potential in expelling hot air through vertical shafts, but its effectiveness is challenged during extreme heat events. These findings underscore the need for adaptive retrofit solutions, such as leveraging existing systems, implementing operational changes, and integrating shading devices to mitigate heat gain. Additionally, the study emphasizes the importance of combining passive strategies with

mechanical systems to enhance energy efficiency and occupant comfort in historic buildings while addressing the anticipated impacts of climate change.

Keywords: Natural ventilation; Historic buildings; Computational Fluid Dynamics; Building preservation; Future weather.

1. Introduction

Greenhouse gas (GHG) mitigation is a pressing global concern with far-reaching impacts on climate and human welfare (Clayton 2021; Jogdand 2020; Philipsborn and Chan 2021; Tonn et al. 2021). Climate change has significantly affected global temperatures, leading to more frequent and intense heat waves and other extreme climate events (Intergovernmental Panel on Climate Change, n.d.; Huang et al. 2020). Specifically, the last decade was the warmest on record, with 2020 ranking as one of the three warmest years so far (WMO, n.d.). Moreover, extreme climate events are predicted to increase in frequency and severity due to global warming, leading to heightened risks of conflict and forced migration (Abel et al. 2019). To anticipate these changes, the Intergovernmental Panel on Climate Change (IPCC) provides various Shared Socioeconomic Pathways (SSP) in its Sixth Assessment Report (AR6) (Lee et al., n.d.; Pirani et al. 2024), with SSP1-2.6 aiming to limit global temperature rise to well below 2°C by 2100, in alignment with the Paris Agreement (Intergovernmental Panel on Climate Change, n.d.). Reducing energy consumption is crucial for achieving these targets, especially in sectors with high energy demands such as buildings (Sharmina 2017; Palermo et al. 2018; Dutta 2021). Particularly, existing buildings play a significant role in global energy consumption and GHG emissions, accounting for over one-third of total energy use and approximately 19% of emissions (Intergovernmental Panel on Climate Change. Working Group III and Edenhofer 2014). Air conditioning systems alone contribute nearly 20% of total building electricity consumption (*Disclaimers Suggested Citation Production Penrose CDB* 2022), and the energy use for space cooling is expected to rise

substantially, potentially becoming the largest electricity consumer in buildings by 2050 (*The Future of Cooling* 2018; Pajek et al. 2024). This underscores the importance of optimizing energy performance in existing buildings, especially those located in cooling dominated climates.

Among the existing building stock, historic buildings represent the pinnacle, but they present unique challenges in energy optimization due to their unique physical and inherent bioclimatic characteristics (Iskandar, Faubel, et al. 2024), as well as stringent preservation requirements (Franzen 2015; Cho et al. 2022a; Ge et al. 2022; Coelho and Henriques 2021; Martinez-Molina and Alamaniotis 2020; Faubel et al. 2024). Moreover, a large number of these buildings have low thermal mass envelopes because they were typically constructed using locally available materials such as wood and lacked any insulation practices. This results in multiple challenges for energy optimization of this heritage building typology. First, low thermal mass buildings have limited capacity to store and regulate heat, which means they can quickly gain or lose heat depending on external temperatures. This characteristic complicates efforts to maintain consistent indoor temperatures and reduces the effectiveness of conventional HVAC systems (Afram et al. 2017). Second, historic preservation mandates prioritize maintaining the authenticity and integrity of original building materials and construction techniques (Pracchi 2014; "The Secretary of the Interior's Standards for the Treatment of Historic Properties - Technical Preservation Services (U.S. National Park Service)," n.d.). Introducing modern insulation materials and techniques can alter the appearance and structural behavior of these buildings, which conflicts with preservation goals (Posani, Veiga, and de Freitas 2021). Additionally, adding insulation to these structures to increase their energy efficiency can cause moisture retention in the wall assembly, which can lead to mold growth and degradation of original materials (National Trust for Historic Preservation, n.d.; Hutkai and Katunský 2021). Therefore, passive cooling

measures need to be investigated as energy-efficient and preservation-appropriate alternatives for this heritage building typology (Webb 2017).

While the preservation of architectural values is paramount, ensuring the thermal comfort of occupants is equally important. Inadequate thermal comfort can lead to reduced occupancy, increased energy consumption, and potential deterioration of the building fabric due to moisture and temperature fluctuations. Furthermore, enhancing thermal comfort contributes to the overall experience of occupants and visitors, thereby increasing the cultural and social value of these historic sites (Martínez-Molina et al. 2016; Fiorito et al. 2022; Kumar, Wright, and Petsou 2024). The main factors affecting thermal comfort in historic buildings include thermal mass, orientation, evaporative cooling, and ventilation. Thermal mass plays a crucial role in regulating indoor temperatures by absorbing heat during the day and releasing it at night (Alwetaishi et al. 2020). However, many historic buildings, particularly in the United States, were constructed using wood-frame structures that lack insulation, resulting in low thermal mass. This makes them more susceptible to overheating, thereby presenting challenges in achieving thermal comfort within these buildings.

Within passive cooling strategies, natural ventilation offers an alternative to reduce energy consumption for cooling and ventilation in buildings (Etheridge 2011; Gilani and O'Brien 2021). This approach is particularly relevant for low thermal mass historic buildings in warm climates, as it is considered one of their inherent sustainable qualities. Utilizing natural ventilation in these structures is deemed a safe method to improve energy efficiency without causing damage to valuable materials or features (Hensley and Aguilar 2011). Therefore, investigating the benefits of natural ventilation for cooling low thermal mass historic buildings in both current and future contexts is crucial to reducing GHG emissions, adapting to future changes in the climate, as well

as ensuring the sustainable conservation of our built heritage and its integration into contemporary society. Historically, natural ventilation served as a primary method for providing thermal comfort in warm climates before the advent of mechanical cooling systems (Martinez-Molina, Williamson, and Dupont 2022). In modern times, with increasing concerns about energy efficiency, climate change, indoor air quality, and historic preservation, natural ventilation strategies have become essential in designing energy retrofits for heritage structures (Iskandar, Bay-Sahin, et al. 2024). These strategies offer an alternative cooling source that reduces energy consumption while enhancing occupants' health, comfort, and productivity (Emmerich, Dols, and Axley, n.d.), and ensure the continued preservation of the built heritage.

Natural ventilation involves the use of natural forces such as wind and buoyancy to bring fresh air from outside into indoor areas (Kopec 2017; Karaiskos, Martinez-Molina, and Alamaniotis 2023; Faubel, Martinez-Molina, and Suk 2024). The concept of Natural Ventilation Potential (NVP) refers to the likelihood of achieving comfortable indoor conditions solely through natural ventilation methods (Luo et al. 2007). NVP assessment is complex and depends on factors such as weather conditions, climate patterns, building design, and surroundings (Yin et al. 2010). Different studies around the world employ various methodologies and criteria to assess NVP, broadly categorized into climate-based and building simulation-based methods (Wang and Malkawi 2019). On the one hand, climate-based approaches provide an overview of NVP using parameters like outdoor air temperature and wind speed, in the absence of detailed building information in early design stages (Wang and Malkawi 2019). For instance, Chen et al. (Chen, Tong, and Malkawi 2017) analyzed global NVP using typical meteorological year (TMY) data and found that temperate climates tend to exhibit higher NVP compared to more extreme climates. Moreover, humidity also played a significant role in NVP assessment, particularly in hot-humid

climates. On the other hand, building simulation tools such as EnergyPlus (EnergyPlusTM, n.d.), DeST (Yan et al. 2008), and IES VE (IES VE, n.d.) allow for a more detailed assessment of NVP by considering specific building design elements and indoor conditions, including internal heat gain, building envelope characteristics, occupancy schedules, and ventilation patterns (Xie et al. 2023). Several studies (Ryan and Sanquist 2012; Royapoor and Roskilly 2015; Fumo, Mago, and Luck 2010; Anđelković, Mujan, and Dakić 2016) have shown that building energy simulation tools can account for uncertainties related to building location and design, and accurately model indoor thermal environments, making them more precise in evaluating NVP than climate-based approaches. However, using appropriate weather data inputs is crucial for accurate building energy simulations (Hensen, n.d.), especially when the aim is to evaluate building energy performance in future years. While different studies have used future weather data in the context of building energy performance and historic preservation (Campagna and Fiorito 2022; Cirrincione, Marvuglia, and Scaccianoce 2021; Bamdad, Matour, Izadyar, and Omrani 2022; Baba et al. 2023; Bienvenido-Huertas et al. 2021; Rajčić, Skender, and Damjanović 2018), none have specifically focused on the impact of natural ventilation strategies as a passive cooling method in hot-humid climates in the context of present and future climate conditions.

Computational Fluid Dynamics (CFD) simulations represent a powerful tool for investigating natural ventilation due to its cost-effectiveness, speed, and accuracy (Zhang, Weerasuriya, and Tse 2020; Jiru and Bitsuamlak 2010). Natural ventilation strategies face a significant challenge in understanding the complex airflow patterns driven by pressure and temperature differentials through wall openings (P.-C. Liu, Lin, and Chou 2009). In this context, CFD models offer a significant advantage in suggesting and predicting the performance of outdoor (Masoumi, Nejati, and Ahadi 2017) and indoor airflow in various natural ventilation strategies.

Unlike field monitoring, CFD simulations can assess multiple ventilation approaches and evaluate airflow in spaces with specific conservation requirements, and thus are widely used in historic buildings analysis (Chassagne et al. 2007; Corgnati and Perino 2013; Balocco and Grazzini 2007; Abuku, Janssen, and Roels 2009; Balocco 2007; Balocco and Grazzini 2009). For example, Bay et al. (Bay, Martinez-Molina, and Dupont 2022) investigated the best natural ventilation approaches for high thermal mass historic buildings located in hot-humid climates and found that night ventilation is the most effective strategy. The study also concluded that mechanical system operation can be reduced in spring and in summer, and that natural ventilation can contribute to occupants' thermal comfort.

Finally, the initial stage of implementing a natural ventilation strategy in a building involves assessing the feasibility and effectiveness of this ventilation strategy. This assessment helps architects select suitable passive or low-energy natural ventilation solutions, ultimately enhancing the energy efficiency of the studied building (Bamdad, Matour, Izadyar, and Law 2022). However, a notable gap in previous research lies in the lack of quantification regarding the effectiveness of natural ventilation as a passive cooling strategy in low thermal mass historic buildings situated in cooling-dominant climates, especially in anticipation of increasingly extreme environmental conditions in the future. This is particularly necessary as such buildings pose challenges for energy retrofits due to their unique construction materials, methods, and stringent preservation requirements, narrowing the options for enhancing the energy efficiency of these structures and providing thermal comfort for their occupants to ensure their continued use and responsible preservation. The lack of prior studies on this topic justifies the current research, which aims to address this gap by examining how current and future climate conditions impact the efficiency of natural ventilation in a low thermal mass historic building in San Antonio, Texas,

USA, a region characterized by a hot-humid climate. Energy and CFD simulations are calibrated with in-situ measured environmental data and used to analyze different natural ventilation strategies, including full capacity natural ventilation, cross ventilation, and stack ventilation. The main goal of this investigation is to guide the selection of the best passive cooling approaches through natural ventilation in historic buildings for present and future use during the current century, ensuring occupants' thermal comfort, preservation of cherished materials and features, and reduction of energy consumption and GHG emissions.

While this study provides valuable insights into the effectiveness of natural ventilation strategies in historic buildings located in a hot-humid climate, it is important to acknowledge certain limitations that may affect the generalizability of the findings. The selected case study is representative of a single historic building construction style, namely low-thermal mass wood-frame structures, which may not fully represent the wide variety of architectural styles, materials, and environmental conditions present in other historic buildings. Consequently, the findings may not be directly applicable to different contexts or building typologies. However, the replicability of the results lies in the detailed methodology employed, which can be adapted and applied to similar buildings with comparable construction and climatic conditions, providing a framework for broader application. Additionally, the study primarily examines natural ventilation in isolation, without considering potential synergies with other passive strategies, such as shading, infiltration reduction, or thermal mass enhancements, that could further improve indoor comfort and energy performance. Furthermore, the impact of external variables, including urban context and wind variability, has not been included in the study to maintain a clear and focused analysis on the specific dynamics of natural ventilation without the potential confounding effects of other variables.

2. Methodology

The methodology employed in this study is depicted in Figure 1 and schematically described as follows. Initially, energy modelling of the case study building was conducted using the IES VE software (IES VE, n.d.), incorporating current building condition drawings and in-situ real data. To ensure the model's reliability before executing energy and CFD simulations, a validation analysis was performed using measured indoor and outdoor environmental data and ASHRAE 14 recommended validation methods (ASHRAE Guideline 14 2014). Future weather data for 2050 and 2080 was generated using the CCWorldWeatherGen (CCWWG) (Jentsch et al. 2013) to assess the impact of changing future climates. Natural ventilation strategies suitable for hot-humid climates were then simulated for present and future climate scenarios, including full-capacity natural ventilation, cross ventilation, and stack ventilation, with a baseline assessment conducted without natural ventilation for comparison with the selected strategies. The resulting environmental conditions were analyzed to evaluate the strategies' efficiency under present and future climate conditions. Finally, CFD simulations were performed for two representative days (spring and summer) during the cooling season, as this period corresponds to the most adverse environmental conditions at the location of the case study building. The outcomes of the CFD simulations allowed for the evaluation of changes in air temperature and air velocity distribution in the case study building throughout the current century.

[Figure 1 near here].

2.1 Building description

The Kelso House, depicted in Figure 2, is a prominent three-story residential structure located north of Downtown San Antonio, Texas, USA, and was selected to serve as the case study for this research. San Antonio sits at an elevation of 240.5 m above sea level and experiences a

climate classified as Cfa-Humid Subtropical with a Bsk-Semi-Arid Climate on its west side (Kottek et al. 2006). The city's temperatures vary significantly throughout the year, averaging 9°C during the coldest months and 32°C during the hottest months. Over the past two decades, the annual average temperature has been 21°C, with summer temperatures peaking at 38°C (US Department of Commerce 2022).

Designed in 1907 by the renowned architect Atlee B. Ayres for Winchester Kelso, a distinguished judge and civic leader (Huddleston 2022), the Kelso House showcases a simplified Neoclassical style with influences from Queen Anne and Craftsman styles, representing prevalent architectural styles from the 19th and 20th century, especially in the United States (Everett 1999a). It holds a place on the National Register of Historic Places as a contributing property to the Monte Vista National Historic District. The building's construction features wood framing, and lacks insulation, making it a representative example of many traditional and historic buildings in the Unites States and around the world (Debailleux 2015). This absence of insulation contributes to its low thermal mass, making it more susceptible to overheating and presenting significant challenges in achieving thermal comfort for its occupants (Kumar, Wright, and Petsou 2024).It also has an irregular and asymmetrical plan, and complex roof proportions. The facades exhibit asymmetrical designs with painted wood teardrop siding, trimmed shingles, wood-frame windows, grand Doric columns, a wood-trimmed entablature with frieze, dentils, cornice, and wood balustrades. A two-story porch wraps around the south and east sides of the house. In 2018, the local Power of Preservation Foundation (PoP) (Power of Preservation Foundation 2022) acquired the property and successfully restored its exterior. While the interior remains in a state of disrepair, the foundation has plans to rehabilitate it in the future. The rehabilitation of this historic structure requires a comprehensive approach aimed at improving energy performance, implementing

strategies for adaptive reuse, and preserving essential historic materials and features. By focusing on this representative case study, the research aims to address broader implications for similar historic buildings facing energy efficiency and thermal comfort challenges, leveraging the replicability of the selected case study.

[Figure 2 near here].

The building's envelope characteristics are detailed in Table 1. The building under study exemplifies a prevalent architectural typology found in historic and existing structures globally, characterized by low thermal mass. Such buildings are prone to overheating and present significant challenges in regulating their indoor environments. Introducing modifications to these structures can compromise the natural climatic response of the envelope, particularly in managing humidity. Moreover, as a historic building, it faces additional constraints related to preserving its historical integrity while implementing any alterations. This context underscores the importance of analyzing the potential effectiveness of natural ventilation cooling for this building typology, both in current and future scenarios.

[Table 1 near here].

2.2 Environmental data collection campaign

A data collection campaign was conducted to assess the current environmental conditions of the building under study, and to serve as a baseline for validating energy and CFD models. A network of 13 indoor data loggers was strategically positioned on the ground floor, first floor, and attic floor, along with 2 outdoor data loggers placed outside the structure. The specifications of the monitoring devices are provided in Table 2. The placement of the data loggers followed ASHRAE Standard 55 ("ANSI, ASHRAE. Standard 55 - Thermal Environmental Conditions for Human Occupancy." 2017) guidelines and is shown in Figure 3. The loggers recorded temperature and

relative humidity both indoors and outdoors during the cooling season, from May to September 2022, and were programmed to capture hygrothermal variables at 15-minute intervals. This setup allowed for comprehensive data collection on the building's environmental conditions and the identification of recurring patterns and significant deviations over the study period. Additionally, the average outdoor wind speed and direction were obtained from the San Antonio International Airport (SAT) weather station for the duration of the monitoring period (Meteostat, n.d.).

[Table 2 near here].

[Figure 3 near here].

The main results of the environmental monitoring campaign are illustrated in Table 3, showing significant temperature fluctuations, with differences between minimum and maximum values ranging between 9°C (September) and 17°C (June). Indoor and outdoor temperatures peaked in July, coinciding with the lowest relative humidity during these months. It is noteworthy that indoor temperatures consistently exceeded outdoor temperatures due to the poor energy efficiency of the existing structure, leading to increased heat gain and retention. However, indoor relative humidity average values remained lower indoor than outdoor throughout the study period. Finally, outdoor air velocity on average was the lowest in September (10.0 km/h) and the highest in May (19.3 km/h), with a prevailing direction of southeast.

[Table 3 near here].

2.3 Natural ventilation strategies

To investigate the impact of present and future climate conditions on natural ventilation efficiency in the studied building, four scenarios were examined during the cooling season (May to September) across three strategically selected periods in the current century: the present, the 2050s, and the 2080s. The choice of ventilation strategies was primarily guided by suggestions

from the building management team, aiming to evaluate the most common natural ventilation methods applied to historic buildings in the geographical area and climate zone of the case study. Additionally, the chosen strategies were identified as the most efficient natural ventilation approaches among commonly used techniques in historic buildings located in hot-humid climate zones (Iskandar, Bay-Sahin, et al. 2024). From a cultural and heritage preservation standpoint, these strategies were also endorsed by local preservation organizations as potential methods for ensuring the preservation of heritage values for this type of historic building.

The natural ventilation strategies investigated in this study are summarized in Table 4 and described as follows (see Figures 3 and 4 for the distribution of all the openings in the building). In Strategy 1 (S1), the building is analyzed without any natural ventilation, with all windows remaining fully closed during the cooling season. This scenario serves as a benchmark for comparing the efficiency of natural ventilation for passive cooling in the case study. Airflow between indoors and outdoors is solely controlled by the building's air infiltration rate. In Strategy 2 (S2), natural ventilation is achieved by keeping all windows fully open 24 hours per day during the cooling season. Strategy 3 (S3) investigates cross ventilation from prevailing winds. During the monitoring campaign, the average outdoor wind direction was south (or southeast). Therefore, cross ventilation from prevailing winds is ensured by keeping all windows on the first and second floors of both the north and south facades fully open 24 hours per day during the cooling season, while the attic access door and windows remain closed consistently. Finally, in Strategy 4 (S4), stack ventilation is achieved by keeping the openings on the first floor and attic fully open 24 hours per day, while those on the second floor remain closed.

[Table 4 near here].

2.4 Estimation of future environmental variables

The energy performance of buildings is greatly influenced by a range of location-specific weather variables, such as dry and wet bulb temperatures, relative humidity, solar radiation, and wind speed and direction (H. Yassaghi, Mostafavi, and Hoque 2019; Hamed Yassaghi, Gurian, and Hoque 2020). This information is stored in weather files, which serve as input data for energy simulation software used to assess and quantify building energy performance. In this study, simulations of indoor environmental conditions in the historic building were conducted using the IES VE software (IES VE, n.d.), which utilizes EnergyPlus Weather (EPW) format files as input parameters.

Typically, weather files are represented as average historical weather data, also known as Typical Year (TY) files, containing values for an entire year based on historical observations summarizing recent weather patterns (Fiocchi, Weil, and Hoque 2014). Among the TYs files, this study relied on the TMY3 (historical data from 1991 to 2005) and the most recent TMYx (2007-2021) for the location of the case study building. These weather files were obtained from the National Renewable Energy Laboratory (NREL) ("National Renewable Energy Laboratory (NREL) Home Page | NREL," n.d.) and the repository for EPW files from the creators of EnergyPlus software ("Climate.Onebuilding.Org," n.d.). Additionally, future weather data were projected using CCWWG (Jentsch et al. 2013), a Microsoft Excel-based weather generator widely used for producing input weather data in building energy performance studies (H. Yassaghi, Mostafavi, and Hoque 2019; Hamed Yassaghi, Gurian, and Hoque 2020; Plaga and Bertsch 2023). The CCWWG employs the 'morphing' technique developed by Belcher et al. (Belcher, Hacker, and Powell 2005), where future weather data is generated by 'shifting' and 'stretching' historical

data from TMY files using climate change projection factors. In shifting, monthly averages of a given parameter within the weather file are shifted while keeping the same variance; conversely, stretching changes the variance of the weather parameter while maintaining the same average. A combination of both shifting and stretching is applied when projecting a weather parameter. Additionally, CCWWG utilizes the Hadley Center Coupled Model Version 3 (HadCM3) of the Atmospheric-Ocean General Circulation Models (GCMs) datasets, along with a given emission scenario, to create future weather data preserving realistic weather sequences for any location. In this study, one of the emission scenarios introduced by the IPCC in the Fourth Assessment Report (4AR) was selected, namely the SRES A2 ("AR5 Synthesis Report: Climate Change 2014 — IPCC," n.d.). The structure of the SRES A2 closely resembles the worst-case scenario for GHG in the atmosphere, which assumes that no further efforts will be made to reduce emissions.

Although newer weather simulation software, such as the Future Weather Generator (FWG) (Rodrigues, Fernandes, and Carvalho 2023), has been developed, the authors validated the use of CCWWG in this analysis by comparing the future environmental conditions obtained for the location of the case study building with those generated by the FWG, which yielded similar results. Finally, it is worth clarifying the nomenclature used by the authors in Section 3, Results. The term *Present* refers to results obtained using the TMY3 and TMYx files, while the term *Future* corresponds to results derived using the weather files generated by CCWWG for 2050 and 2080. In this case, the future years do not represent exact dates but encompass monthly average values for the weather files during the following periods: from 2040 to 2069 for 2050, and from 2070 to 2099 for 2080, respectively ("HadCM3 Climate Scenario Data," n.d.).

2.5 Energy and CFD modeling and validation

CFD is a numerical simulation method used to model fluid flow and heat transfer processes within a computational domain. It involves solving the governing equations of flow, including momentum, energy, turbulence, scalar/mass fraction, and mass continuity, within a domain divided into small volumes called cells, which collectively form a grid. Linear equations are applied to each cell, creating a system of equations that is iteratively solved to determine variable values and investigate heat transfer processes and airflow patterns.

Various modules within the IES VE software (IES VE, n.d.) were used to run the energy and CFD simulations, including ModelIt, MacroFlo, MicroFlo, and VistaPro. The features of each module are described as follows: i) ModelIt was used to define building parameters and site properties including model geometry, building orientation, window-to-wall ratio, and construction materials, as detailed in Table 5. The case study building modelled in the IES VE software is shown in Figure 4. All the parameters used in the simulation software were meticulously collected under real-world conditions to ensure accurate and realistic outcomes; ii) MacroFlo module employs a zonal airflow model to calculate bulk air movement within and through the building to analyze infiltration and natural ventilation. Input data pertaining to the historic building openings and their characteristics (e.g., exposure types, percentage, and degree of opening, and daily, weekly, or yearly modulating profiles) were defined, and different ventilation profiles were created for each one of the strategies listed in Table 4. Additionally, the air infiltration rate of the whole envelope was set to 2.032 l/(s m^2) in the simulations, considering the case study building as a leaky construction. This value for the air infiltration was based on both proposed rates for historic buildings and the low levels of airtightness usually associated with detached houses, such as the case study (Cho et al. 2022b; Tiberio and Branchi 2013); iii) VistaPro module (Integrated

Environmental Solutions Limited (IES), n.d.) was used to simulate the indoor environmental data needed to compare the different ventilation strategies; iv) MicroFlo module ("CFD: MicroFlo User Guide IES VE 2015," n.d.) was used to generate the final CFD graphs by importing boundary conditions from VistaPro. Apache Energy Simulation results were used to set wall and window surface temperatures as boundary conditions for the CFD model in MicroFlo which is a steady state analysis tool.

[Table 5 near here].

[Figure 4 near here].

The CFD simulations were run for the natural ventilation strategies listed in Table 4 on two representative days during the cooling season using the present, 2050, and 2080 weather data. Since the cooling period ranged from May to September, encompassing both spring and summer, a representative day of each season was chosen to assess the overall performance of the natural ventilation strategies. Specifically, the representative days selected in this analysis were May 8th (spring) and July 23rd (summer) as ventilation rates were high. 12:00 pm was selected for the CFD simulations due to its alignment with peak solar radiation and outdoor temperatures, enabling the assessment of the building's behavior under extreme thermal loads and facilitating straightforward comparisons between the ventilation strategies. This time allows for the analysis of the building's response to peak thermal loads, which can be crucial for understanding its performance under extreme conditions (Fatnassi et al. 2023; Bay, Martinez-Molina, and Dupont 2022). Additionally, 12:00 pm is a convenient time for comparisons between the different ventilation strategies, as it provides a consistent reference point for evaluating changes in temperature and airflow patterns. To avoid the influence of external factors on the assessment of natural ventilation for passive cooling, the simulations were performed with the structure in its free-floating state, i.e. without mechanical ventilation systems installed and with no presence of occupants (occupancy set to 0).

Regarding the boundary conditions for the CFD model, wall surface temperatures in present scenarios were defined as 27.9°C (May 8th) and 39°C (July 23rd), while window temperatures were 28.1°C (May 8th) and 40.1°C (July 23rd). In the 2050 scenarios, these values were 31.5°C and 45°C for wall surface temperatures, and 31.7°C and 45.3°C for window surface temperatures. For the 2080 scenarios, the wall surface temperatures reached 36°C (May 8th) and 47.1°C (July 23rd), and the window surface temperatures were defined as 36.1 (May 8th) and 47.9°C (July 23rd). The surface temperatures for CFD boundary conditions of the models are exported by Apache which is a dynamic thermal simulation program that utilizes first-principles mathematical modeling to simulate heat transfer processes within and around a building. The simulation uses real weather data and can cover any period from a day to a year, tracking the building's thermal conditions at intervals as small as one minute. The initial surface temperatures are established based on the boundary conditions obtained from Apache results using the Vista application. By selecting the thermal zone to be simulated in CFD, the boundary conditions are imported through the "Import boundary data" feature. So, the following parameters of the boundary conditions are automatically assigned to the model: i) all surface (wall, window, door and hole) temperatures, ii) flows through MacroFlo openings, and iii) convective component of the internal gains (instantaneous additions of heat to the zone air) specified in the room template of Apache.

In the CFD settings, discretization scheme is defined as Upwind scheme. Additionally, the standard k-e turbulence model was used in MicroFlo to assess the grid cell's turbulent viscosity throughout the calculation domain. This turbulence model is widely used in the related literature providing accurate results in the context of CFD investigations (Savicki, Goulart, and Becker 2021; Ramdlan et al. 2016; IESVE 2021), so it was chosen as the default model in the selected software.

The default grid spacing and merge tolerance are established in Table 6. The merge tolerance allows grid lines that are closer than the specified tolerance to be combined into a single line, reducing unnecessary gridding. The system grid was defined in the x, y, and z directions using three grid constraints. In CFD applications, computational grid cells define the solution domain, with the number and size of the cells determining the resolution of the calculation. Since this study analyses internal flow inside the different areas of the building, the computational domain is confined within the geometrical boundaries of the building. Boundary conditions are applied directly to these surfaces. Setting the minimum opening flow rate to 0.0001 m^3/s, the inlet air velocity conditions were imported into the CFD module from Apache energy simulation results, and the data for each inlet were interpreted using the generated CFD graph. Additionally, the CFD grid was created with the maximum cell aspect ratio under 12:1 to ensure a high level of resolution. The grid cells defined for each model were as follows: the first floor (horizontal section from 1.5 m) with 3,266,856 cells, the second floor (horizontal section from 5.5 m) with 3,363,890 cells, and the first floor with the staircase (vertical section) with 3,487,655 cells. Cells can vary in size and are typically categorized as increasing, decreasing, or uniform. Smaller and uniform grid cells are usually defined in areas with significant solution gradient variables. For efficiency in computing time, it is common to vary the grid size spatially, increasing or decreasing it away from critical areas. Due to the grid limitations in MicroFlo, which make it challenging to incorporate complex forms, the modeled building was kept simple to avoid exceeding the maximum aspect ratio (Table 6).

Convergence criteria are predefined limits in CFD simulation software that indicate when a numerical solution for a set of equations has reached a stable value. In this study, a total of 2,000 iterations per simulation was set in IES VE. Additionally, the convergence of the numerical

solutions in each CFD simulation was assessed through the residuals of the solutions provided by the software, which ranged from 10-5 to 10-4. These are typical values associated with the convergence of solutions in CFD simulations (Sørensen and Nielsen 2003; IESVE 2021).

[Table 6 near here].

Finally, the case study building modelled in IES VE software was validated using the indoor air temperature and relative humidity measurements from the environmental data collection campaign. The validation variables were selected based on the research's objectives, focusing on analyzing the impact of various natural ventilation scenarios on indoor conditions and occupant comfort. These variables are also reliable in ensuring validation robustness, and are utilized in many similar research studies to validate CFD models (Lerma et al. 2021; Pérez-Vega et al. 2021; Bay, Martinez-Molina, and Dupont 2022; Yohana et al. 2017; Iskandar, Bay-Sahin, et al. 2024). The measured data from the monitoring campaign and the simulated values yielded by the VistaPro module were both at the testing height of 1.10 m, in accordance with ASHRAE Standard 55 ("ANSI, ASHRAE. Standard 55 - Thermal Environmental Conditions for Human Occupancy." 2017) guidelines for consistency between seated and standing occupants. Although the validation was performed for the entire cooling season, Figure 5 depicts the simulated and measured values of indoor air temperature and relative humidity during the selected representative days (and one day prior) for the CFD simulations: May 7th and May 8th in spring, and July 23rd and July 24th in summer.

[Figure 5 near here].

Uncertainty indices, including normalized mean biased error (NMBE) and coefficient of variation of the root mean square error (CV(RMSE)), were calculated as per ASHRAE Guideline 14 (ASHRAE Guideline 14 2014) by means of Eqs. (1) and (2):

$$\mathrm{NMBE}\ (\%) = \frac{1}{\overline{\mathrm{Y}}} \frac{\sum_{\mathrm{i}=1}^{\mathrm{N}} \left(\mathrm{Y_i} - \hat{\mathrm{Y}}_\mathrm{i}\right)}{\mathrm{N} - \mathrm{p}} \times 100\,, \#(1)\#$$

$$\mathrm{CV(RMSE)}\ (\%) = \frac{1}{\overline{\mathrm{Y}}} \sqrt{\frac{\sum_{\mathrm{i}=1}^{\mathrm{N}} \left(\mathrm{Y_i} - \hat{\mathrm{Y}}_\mathrm{i}\right)^2}{\mathrm{N} - \mathrm{p}}} \times 100\,.\ \#(2)\#$$

In this context, Y_i represents the measured value for the indoor air temperature and relative humidity, $\hat{\mathrm{Y}}_\mathrm{i}$ stands for the simulated value for the same variables given by IES VE software, and $\overline{\mathrm{Y}}$ corresponds to the average of measured values Y_i. Moreover, N is the total number of data points used in the analysis, and p denotes the modifiable model parameter. ASHRAE recommendations for hourly validation are NMBE and CV(RMSE) not to exceed ±10% and 30%, respectively. The results of the validation are summarized in Table 7, meeting ASHRAE's requirements, thus validating the model predictions and indicating the model's reliability and accuracy. It is worth noting that the model was also validated for the entire cooling season, and the metrics NMBE and CV(RMSE) were within the accepted ASHRAE recommendations, although only the selected representative days are depicted for simplicity.

[Table 7 near here].

3. Results

In this section, the results of the energy simulations are investigated. Hourly indoor environmental conditions in the historic building were simulated for the various ventilation strategies outlined in Table 4. Three different weather files corresponding to the structure's location in the present, 2050, and 2080 were employed in the simulations to quantify and assess the effectiveness of these strategies during the cooling season, namely from May to September. Additionally, two representative days, May 8th, and July 23rd, were selected for spring and summer for CFD analysis of temperature and air velocity distribution throughout the building.

3.1 Environmental data analysis

3.1.1 Weather conditions in San Antonio during the cooling season

The results for outdoor environmental variables, depicted in black in Figure 6 (numerical values summarized in Table 9), exhibited consistent trends throughout the current century for the case study location, with differences in recorded values. Present weather data showed the lowest air temperatures at the beginning and end of the cooling season, with an upward trend from May to July, followed by a decrease from July to September. Monthly averages were 24.9°C, 27.2°C, 29.6°C, 27.7°C, and 24.5°C from May to September, respectively (Figure 6 i-a). This trend persisted in 2050 and 2080, with an overall increase of 4°C and 7°C on average in 2050 and 2080, respectively, compared to present weather data (Figure 6 i-b and i-c). The highest monthly average outdoor air temperatures were 34.1°C and 36.6°C in July 2050 and July 2080, respectively. Outdoor air relative humidity remained relatively constant around 70% throughout the cooling season in present weather data, except for lows and highs in July (58.8%) and September (76.3%), respectively (Figure 6 ii-a). Similar trends were observed in 2050 and 2080, with an overall decrease in monthly average relative humidity of approximately 10% and 20% in 2050 and 2080, respectively, compared to present weather data (Figure 6 ii-b and ii-c). The lowest relative humidity levels were recorded in July in both 2050 (45.8%) and 2080 (39.8%).

Finally, wind speed and direction are critical factors for evaluating the impact of natural ventilation strategies for passive cooling in buildings without mechanical ventilation systems, such as the historic structure in this study. Present weather data showed relatively constant wind speeds in May and June at 2.2 m/s, with the highest recorded value in July at 3.4 m/s (Figure 6 iii-a). Monthly average wind speeds then decreased in August and September to around 2.5 m/s. A similar pattern was observed in 2050 and 2080, with significant differences in values, particularly

in July and August of both years (Figure 6 iii-b and iii-c). The highest values reached around 4 m/s in July 2050 and slightly exceeded this value in July 2080, while the monthly average in August was about 3.2 m/s in both years.

3.1.2 Simulated results during the cooling season

The simulated results for the indoor environmental variables are depicted in Figure 6 (numerical values summarized in Table 9) for each of the natural ventilation strategies listed in Table 4, and for both present and future weather data, as average of the entire building. The difference between the value of a studied environmental factor in 2050 or 2080 weather data and its value in the present weather data is represented by $\Delta x = x_{2050,\,2080} - x_{Present}$, where x stands for temperature (T), relative humidity (RH), air velocity (v_{air}), and ventilation rate (Q).

The impact of natural ventilation on passive cooling is evident, with S1 exhibiting the highest indoor air temperature compared to the other strategies throughout the entire cooling season in both present and future scenarios (Figure 6 i-a). The monthly average for May and September in the current weather data for S1 was about 30°C, while the middle months of the cooling season reached almost 36°C. S2,S3, and S4 followed the same trend and similar values as the outdoor average monthly temperatures (section 3.1.1). Although the indoor air temperatures for S2, S3, and S4 were very similar, there was an overall decrease of about 5°C compared to S1 (Figure 6 i-a). For 2050 and 2080, all four natural ventilation strategies exhibited the same pattern as the outdoor average monthly temperatures, with higher values compared to the present temperature data. The highest indoor air temperatures were recorded in July 2050 and July 2080 for S1, reaching around 40°C (ΔT = 5°C) and 43°C (ΔT = 7°C), respectively (Figure 6 i-b and i-c). In contrast, the lowest values in S1 were recorded at the beginning and end of the cooling period, around 33°C in 2050 (ΔT = 3°C), and around 36°C in 2080 (ΔT = 6°C). For S2, S3 and

S4, the highest temperatures reached 35°C (ΔT = 5 °C) and 37°C (ΔT = 7°C) in July 2050 and July 2080, respectively, while the lowest values were observed in both May and September at 28°C in 2050 (ΔT = 3°C) and 31°C in 2080 (ΔT = 6°C).

Similarly, indoor air relative humidity was heavily impacted by the natural ventilation strategies. For the present weather data, indoor air relative humidity in S1 remained relatively constant around 50% throughout the cooling season, except for lows and highs in July (39.7%) and September (58.5%), respectively. S2, S3, and S4 exhibited similar pattern and values, closely following outdoor relative humidity conditions (section 3.1.1). For the future weather data, all four ventilation strategies also followed the same pattern. Interestingly, the general trend for average indoor relative humidity in both 2050 and 2080 was opposite to that of average indoor temperature, with relative humidity decreasing as temperature increased. The pattern in each of the two studied years mirrored that of the corresponding outdoor conditions, with S2, S3, and S4 exhibiting almost identical indoor and outdoor air relative humidity values. In 2050 and 2080, S1 consistently maintained the lowest indoor air relative humidity compared to the different ventilation strategies, with an average difference of 12% between S1 and the other scenarios throughout the entire cooling season (Figure 6 ii). Generally, indoor relative humidity values were lower in 2050 and 2080 compared to the present data, with an average decrease of ΔRH = -8% in 2050 and ΔRH = -13% in 2080.

Finally, the ventilation rates were also investigated for S2, S3 and S4 where natural ventilation is in effect. For the different years, S3 yielded the highest ventilation rates, followed by S4, then S2 (Figure 6 iv). Specifically, the highest values for S3 were observed at 1,010 l/s in July (present), 1,070 l/s in July 2050, and 1,116 l/s in July 2080, respectively. The ventilation rate trends for S2 and S4 were very similar in the three years investigated in this study, with values

ranging from 105 l/s to 668 l/s, and no significant fluctuations between present and future weather data. The highest values in both ventilation strategies were obtained in the middle of the cooling season, namely in July, and the lowest in May and September, following the same trend as the outdoor wind speeds (Figure 6 iii). S3 followed this same trend in the three analyzed periods.

[Figure 6 near here].

3.2 CFD results for two representative days during the cooling season

3.2.1 Results for the present weather data

For the present weather data, the simulated results for May 8th and July 23rd are depicted in Figures 7 and 8, respectively. The highest average indoor air temperature was recorded in S1 on both May 8th (28.8 °C, Table 8) and July 23rd (33.2 °C, Table 8), with no air movement occurring inside the building. Due to thermal stratification, temperatures on the second floor were consistently about 1°C higher than those on the first floor in both seasons (Figures 7a-b and 8a-b). However, the air temperature distribution on each floor was overall uniform. Finally, the stack effect caused the lowest air temperature at the bottom of the staircase on both days (Figures 7c and 8c).

In S2, the average indoor air temperature was 26.4°C on May 8th and 30.2°C on July 23rd (Table 8), representing a decrease of 2.4°C and 3°C compared to S1 for the two days, respectively. Airflow near the windows resulted in consistently lower temperatures in those areas compared to other zones on the same floor (Figures 7d-e and 8d-e). Indoor air velocity, depicted in Figures 7f and 8f, was higher on May 8th (up to 1.65 m/s) than on July 23rd (up to 0.75 m/s) resulting in more pronounced temperature variations on May 8th, while the indoor air temperature distribution on July 23rd was more uniform throughout the building. On May 8th, rooms with lower air temperatures were located in the prevailing wind direction, namely southeast. It is important to

note that wind velocity was lower near windows shaded by the porch. However, the shaded rooms, particularly the living room (see Figure 3 for the distribution of the spaces within the building), maintained the lowest temperatures throughout the building due to the porch's impact in reducing mean radiant temperatures from solar radiation (Figure 7d).

S3 achieved lower average indoor air temperatures compared to S2, with values of 25.6°C on May 8th (0.8°C lower than S2) and 29.1°C on July 23rd (1.1°C lower than S2). This strategy involved opening windows on the north and south facades to create an airflow in the dominant direction of the prevailing winds (Table 3), which contributed to replacing the interior warm air with fresher outside air and thus achieving comfort ventilation (Figures 7i and 8i). This airflow reduced indoor air temperatures on both representative days, particularly in the areas near the open windows (Figures 7g-h and 8g-h). Interestingly, the second floor exhibited slightly higher temperatures in S3 than in S2, while the first floor was consistently cooler in S3. The impact of cross ventilation on indoor air temperature in S3 was more pronounced on May 8th than on July 23rd due to the higher air velocity resulting in a more uniform indoor air temperature distribution throughout the building on July 23rd (Figures 8g-h-i).

In S4, the average indoor air temperature was 25.7°C on May 8th and 29.7°C on July 23rd (Table 8), achieving temperatures similar to those in S3 and lower values than S2 and S1. Stack ventilation is based on density and pressure differences between hot and cold air; hot air rises while cold air moves downward, creating a current due to air temperature differences. On the two days analyzed, the airflow created towards the attic through the staircase (Figures 7l and 8l) contributed to lowering the air temperature in exposed areas (Figures 7j-k and 8j-k). The coolest area on both floors on May 8th was consistently the staircase (Figures 7j-k). Lower temperatures were also observed in the first-floor rooms, especially in the shaded living room, even though air movement

was slower near the shaded windows. The bedrooms on the second floor in S4 exhibited higher temperatures compared to S2 and S3 but remained cooler than in S1 (Figures 7b-e-h-k). On July 23rd, the airflow created by stack ventilation, although with faster air velocity near the staircase (Figure 8l), did not significantly alter the air temperature distribution in the building (Figures 8j-k). Interestingly, temperatures on the second floor were slightly lower than on the first floor and than in S2 and S3 in this case (Figures 8e-h-j-k).

[Figure 7 near here].

[Figure 8 near here].

[Table 8 near here].

3.2.2 Results for the future weather data

For the future weather data, the simulated results for May 8th and July 23rd are depicted in Figures 9 and 10 for 2050, and Figures 11 and 12 for 2080, respectively. The results for S1 showed an average indoor air temperature of 30.2°C in spring 2050 (ΔT = 1.4°C), 33.8°C in spring 2080 (ΔT = 5.0°C), 43.0°C in summer 2050 (ΔT = 9.8°C), and 45.5°C in summer 2080 (ΔT = 12.3°C), representing the highest values among the simulated air temperatures for the different ventilation strategies (Table 8). Temperature distribution in this case was similar to that in present weather data, except for cooler temperatures observed in the staircase on May 8th, 2050 (Figure 9c). A similar impact was noted on May 8th, 2080, but it was less pronounced (Figure 11c).

The outcomes for S2 showed an average indoor air temperature of 28.7°C in spring 2050 (ΔT = 2.3°C), 32.9°C in spring 2080 (ΔT = 6.5°C), 39.3°C in summer 2050 (ΔT = 9.1°C), and 42.0°C in summer 2080 (ΔT = 11.8°C); numerical values summarized in Table 8. In 2050 and 2080, the air velocity in spring was significantly lower than in present weather data (Figures 7f, 9f and 11f), with air movement perceived almost exclusively near the east facade windows (Figures

9f and 11f), while in present weather data, the air velocity was considerable near south-facing windows as well. This, coupled with higher outdoor temperatures in both future studied years, resulted in higher indoor air temperatures near the windows than those measured in other zones on the same floor, opposite to results obtained for the present weather data (Figures 7d-e, 9d-e, and 11d-e). This also caused the warmest rooms to be those aligned with the east wind direction and not shaded, namely the dining room and the east bedroom. On the representative summer day in 2050 and 2080, air velocities were lower than in spring, and outdoor temperatures were much higher (up to 9°C higher than in spring), resulting in a more even distribution of indoor temperatures, with higher values perceived near the east-facing windows and in unshaded east-oriented rooms, similar to spring.

The results for S3 showed an average indoor air temperature of 28.4°C (ΔT = 2.8°C) in spring 2050, 32.4°C in spring 2080 (ΔT = 6.8°C), 39.2°C in summer 2050 (ΔT = 10.1°C), and 41.9°C in summer 2080 (ΔT = 12.8 °C); numerical values summarized in Table 8. On the representative spring day, the indoor air velocity in both studied years was significantly lower near the south windows compared to the results for the present weather data (Figures 7i, 9i, and 11i), resulting in a more even indoor temperature distribution. The coolest zone in the building was the living room due to the shade provided by the porch (Figures 9g and 11g), and the second floor was significantly hotter than the first floor, especially in 2080 (Figures 9g-h and 11g-h). On the summer representative day, low air velocity was perceived in both future studied years, similar to the present weather data, resulting in similar uniform indoor air temperature distribution. However, the higher outdoor temperatures in the future years caused no visible difference in indoor temperatures between the first and second floors, opposed to the case with the present data.

In S4, the average indoor air temperature was 27.9°C in spring 2050 (ΔT = 2.2°C), 31.7°C in spring 2080 (ΔT = 6.0°C), 39.3°C in summer 2050 (ΔT = 9.6°C), and 41.9°C in summer 2080 (ΔT = 12.2°C); numerical values summarized in Table 8. On the spring representative day of both studied future years, the airflow created towards the attic through the staircase contributed to lowering the air temperature in the exposed areas on the first floor (Figures 9j-l and 11j-l). The warmer outside air entering through the east-facing windows resulted in an increase in indoor air temperatures near these windows on the first floor (Figures 9j and 11j). However, the shaded living room remained cooler than the non-shaded dining room, even though they both have east-oriented windows. Due to lack of ventilation on the second floor, temperatures were evenly distributed and higher than on the first floor. On the summer representative day of both 2050 and 2080, the air velocity was extremely low and air temperature distribution was uniform throughout the building (Figures 10j-k-I and 12j-k-l).

[Figure 9 near here].

[Figure 10 near here].

[Figure 11 near here].

[Figure 12 near here].

4. Discussion

The complexity of hot-humid climate zones and anticipated increase in temperatures in the next years have often resulted in the incorporation of very invasive mechanical systems in existing buildings to meet occupants' thermal comfort needs ("ANSI, ASHRAE. Standard 55 - Thermal Environmental Conditions for Human Occupancy." 2017). In historic buildings, this approach is very problematic as it can cause irreparable damage to unique materials and features and cause unwanted problems such as moisture buildup in the envelope materials since these buildings were

not originally designed to host mechanical systems (National Trust for Historic Preservation, n.d.). Exploring passive strategies for cooling historic buildings in the present and future is necessary in this context to combine the requirements of historic preservation with those of energy efficiency and thermal comfort enhancements. Since natural ventilation is one of the most efficient passive cooling strategies in hot-humid climates (Nagasue et al. 2024), this paper investigated the potential of different natural ventilation approaches in cooling a historic residential building located in such a climate, both in the present and in future years in this century (2050 and 2080).

Since the building is constructed with low-thermal mass materials, namely wood, the impact of the outdoor environmental conditions is prominent on the indoor environment, as shown in the simulated environmental data results. Moreover, these structures are more prone to high heat gains through solar radiation, which can increase indoor temperatures significantly, sometimes surpassing outdoor temperatures due to heat retention. Numerous and large operable windows were typical in historic buildings to maximize ventilation and help improve thermal comfort (Everett 1999b; Hensley and Aguilar 2011). The airflow created by the opening of the windows mitigates heat buildup by allowing fresh outside air to enter the building and renew the present one. In this case study, the three investigated natural ventilation strategies, namely ventilation at full capacity, cross ventilation, and stack ventilation, were all successful in lowering indoor temperatures significantly compared to the baseline scenario S1 where no ventilation was in effect (about 5°C decrease), in both the present and future studied years, indicating the effectiveness of these strategies in this context. However, this impact was less pronounced compared to the outdoor conditions, suggesting that natural ventilation strategies may struggle to maintain indoor comfort levels when external temperatures are uncomfortable. Moreover, higher indoor relative humidity values were perceived in the three studied strategies compared to the baseline scenario S1 (up to

16% increase), but consistently always lower than outdoor levels in all strategies. High relative humidity values can be problematic in historic buildings as moisture buildup can negatively impact thermal comfort as well as materials conservation (Yuk et al. 2023), but the studied strategies proved to be successful in decreasing the indoor values at least below the high outdoor values, in the present and future studied years.

Interestingly, the environmental data showed a close correlation between outdoor air velocity and indoor ventilation rates. When the monthly environmental data is analyzed, no strict correlation can be perceived between indoor ventilation rate and indoor air temperature or relative humidity values, as the highest ventilation rates were always recorded in S3, while the lowest indoor air temperatures were achieved by S2, and the lowest indoor relative humidity values were reached in S4. However, in the analysis of the two representative days, a close relationship was observed between indoor ventilation rates and indoor temperature. The highest indoor ventilation rates were often coupled with the lowest average indoor temperatures in the building, with S3 being the most efficient strategy in lowering average indoor temperatures on both the spring and summer representative days.

Moreover, the CFD analysis illustrated a relationship between air velocity and indoor temperature distribution, as higher air velocities resulted in higher or lower indoor temperatures in the exposed areas than in other areas of the building, while low air velocities caused more uniform temperature distributions. Lower indoor temperatures were recorded only in the present weather data when outdoor temperatures were moderate. However, in 2050 and 2080, higher outdoor temperatures were recorded (up to 4.5°C higher in 2050 and 7.3°C higher in 2080). In this case, high air velocity resulted in an increase in the indoor temperatures of the exposed areas. As the prevailing wind direction in San Antonio during the monitoring campaign was southeast, with a

dominant south orientation, south and north windows were open in S3 to examine the impact of cross ventilation through the most influential wind direction. The environmental and CFD simulation results showed that the deep porch reduced air velocity from the south orientation, aligning with findings from Argiriou et al.'s study on the effect of shading devices on airflow across large openings in natural ventilation (Argiriou, Balaras, and Lykoudis 2002). Higher air movement was noted near east-oriented windows, particularly those unshaded by the porch. Despite this reduction in air velocity, indoor temperatures were consistently lower in the shaded rooms compared to unshaded rooms with higher air velocity. This underscores the greater impact of heat gains through solar radiation compared to air velocity, particularly in low-thermal mass buildings.

The accumulative analysis of environmental and CFD simulated data can provide invaluable information on the impact of natural ventilation strategies both in the present and in the future. While all natural ventilation strategies were successful in decreasing indoor temperatures compared to no natural ventilation, their impact is only positive when outdoor temperatures are moderate. In the adverse climate conditions of San Antonio, especially in summer, natural ventilation is not sufficient to provide thermal comfort and ensure the conservation of historic materials and features in the present or future. Therefore, a mixed-mode ventilation system can be considered to lower the energy consumption of the building, especially in spring. Among the natural ventilation strategies, cross ventilation proved to yield the highest indoor ventilation rate and lowest indoor temperatures compared to other natural ventilation strategies. Stack ventilation was the most efficient in decreasing relative humidity values, but high temperatures were consistently observed on the second floor. This strategy can be efficient during the day, when relative humidity values are high and the bedrooms on the second floor are not in use.

It is important to acknowledge that this study focused solely on natural ventilation, excluding potential synergies with other passive strategies, to maintain a focused analysis of its specific dynamics without introducing confounding effects. However, combining multiple passive cooling strategies can significantly improve occupants' thermal comfort, reduce energy consumption, and enhance the preservation of historic buildings. For instance, (S. Liu et al. 2020) highlighted the critical role of airtightness and solar shading in maximizing indoor thermal comfort and minimizing energy consumption under future climate scenarios in hot and humid conditions. Additionally, (Azmi et al. 2023) emphasized the importance of improving the building envelope's thermal performance to mitigate thermal loads from the external environment, as well as encouraging occupants to actively operate passive systems, such as opening windows or using fans, instead of relying on HVAC systems. Therefore, future research should explore the combined effects of various passive strategies to provide a more comprehensive analysis of passive cooling in historic buildings.

5. Conclusion

The built heritage constitutes a considerable and valuable stock that requires specific care to enhance energy efficiency, ensuring its continued use and reducing GHG emissions resulting from poor energy performance or the demolition of these structures. It also has unique architectural and environmental characteristics and entails specific preservation requirements, which makes the exploration of passive retrofit approaches extremely necessary. Particularly, low thermal mass historic buildings are notably sensitive to outdoor environmental conditions and face constrained options for energy retrofit solutions due to strict preservation mandates. Additionally, they may encounter challenges related to maintaining material structural and architectural integrity which narrows the selection of suitable retrofit strategies. Natural ventilation is deemed a safe passive

cooling approach for this building typology, but previous research has overlooked the effectiveness of various natural ventilation strategies in cooling these buildings, especially under anticipated future climate conditions. This study aims to fill this gap by analyzing the climatic potential of different natural ventilation strategies as a passive cooling approach in a historic residential case study, particularly in a hot-humid climate. The investigated potential includes the present as well as two future periods in this century, namely 2050 and 2080, and the selected strategies were natural ventilation at full capacity, cross ventilation, and night ventilation. An environmental monitoring campaign was performed to gather in-situ environmental data, which served to validate energy and CFD models used to conduct the analysis. CCWWG was used to generate future weather files to simulate the potential of the selected natural ventilation strategies in the upcoming years.

It was found that all three strategies are successful in significantly lowering indoor temperatures compared to a baseline scenario with no ventilation. However, the impact of natural ventilation strategies is less pronounced compared to outdoor conditions, suggesting challenges in maintaining indoor comfort levels when external temperatures are uncomfortable, particularly in summer and in the future. Despite this, the strategies prove successful in decreasing indoor relative humidity values, which can be problematic in historic buildings. A close correlation was also perceived between outdoor air velocity and indoor ventilation rates as well as between indoor ventilation rate and average indoor air temperature. Moreover, higher air velocities caused a decrease in indoor temperatures in ventilated areas when outdoor temperatures were moderate, while producing the opposite impact when outdoor temperatures were high. Lower air velocities usually resulted in a uniform distribution of indoor temperatures. The study suggests that natural ventilation strategies can enhance energy efficiency in historic buildings, while preserving their

unique characteristics. Unfortunately, natural ventilation alone is not sufficient to ensure thermal comfort throughout the entire cooling season, which indicates the potential necessity of a mixed-mode ventilation system, especially in the face of climate change.

Future research could further refine these strategies for different historic building typologies and explore their integration with other sustainable technologies. Long-term monitoring of buildings implementing these strategies could provide valuable insights into their effectiveness and durability over time. Finally, the findings of this study offer valuable insights into selecting optimal passive cooling methods, particularly through natural ventilation, for both current and future application in historic buildings throughout the present century. This includes ensuring occupants' thermal comfort, preserving the historical integrity of the buildings, and decreasing energy consumption and GHG emissions. Additionally, these findings contribute to the development of a more resilient stock of historic buildings capable of addressing potential challenges arising from increasing temperatures due to climate change. The methodology employed in this research is designed to be replicable and adaptable, making it applicable to numerous low thermal mass historic buildings in hot-humid climates worldwide.

Acknowledgments

This research would not have been possible without the cooperation of the Power of Preservation (PoP) Foundation. The authors would also like to acknowledge Assaad Akle and Panos Karaiskos for their support in the environmental monitoring campaign.

Appendix A

The numerical results of the environmental variables obtained to assess the impact of the different natural ventilation strategies on passive cooling in the case study building are summarized in Table 9. Specifically, this table contains the monthly average of the environmental variables

during the cooling season, including indoor and outdoor air temperature and relative humidity, and indoor ventilation rates.

[Table 9 near here].

Data availability statement

The data that support the findings of this study are available from the corresponding author upon reasonable request.

References

Abel, Guy J., Michael Brottrager, Jesus Crespo Cuaresma, and Raya Muttarak. 2019. "Climate, Conflict and Forced Migration." *Global Environmental Change* 54 (January):239–49. https://doi.org/10.1016/j.gloenvcha.2018.12.003.

Abuku, Masaru, Hans Janssen, and Staf Roels. 2009. "Impact of Wind-Driven Rain on Historic Brick Wall Buildings in a Moderately Cold and Humid Climate: Numerical Analyses of Mould Growth Risk, Indoor Climate and Energy Consumption." *Energy and Buildings* 41 (1): 101–10. https://doi.org/10.1016/j.enbuild.2008.07.011.

Afram, Abdul, Farrokh Janabi-Sharifi, Alan S. Fung, and Kaamran Raahemifar. 2017. "Artificial Neural Network (ANN) Based Model Predictive Control (MPC) and Optimization of HVAC Systems: A State of the Art Review and Case Study of a Residential HVAC System." *Energy and Buildings* 141 (April):96–113. https://doi.org/10.1016/J.ENBUILD.2017.02.012.

Alwetaishi, Mamdooh, Ashraf Balabel, Ahmed Abdelhafiz, Usama Issa, Ibrahim Sharaky, Amal Shamseldin, Mohammed Al-Surf, Mosleh Al-Harthi, and Mohamed Gadi. 2020. "User Thermal Comfort in Historic Buildings: Evaluation of the Potential of Thermal Mass, Orientation, Evaporative Cooling and Ventilation." *Sustainability (Switzerland)* 12 (22): 1–24. https://doi.org/10.3390/su12229672.

Anđelković, Aleksandar S., Igor Mujan, and Stojanka Dakić. 2016. "Experimental Validation of a EnergyPlus Model: Application of a Multi-Storey Naturally Ventilated Double Skin Façade." *Energy and Buildings* 118 (April):27–36. https://doi.org/10.1016/j.enbuild.2016.02.045.

"ANSI, ASHRAE. Standard 55 - Thermal Environmental Conditions for Human Occupancy." 2017.

"AR5 Synthesis Report: Climate Change 2014 — IPCC." n.d. Accessed April 23, 2024. https://www.ipcc.ch/report/ar5/syr/.

Argiriou, Athanassios A., Constantinos A. Balaras, and Spyridon P. Lykoudis. 2002. "Single-Sided Ventilation of Buildings through Shaded Large Openings." *Energy* 27 (2): 93–115. https://doi.org/10.1016/S0360-5442(01)00058-5.

ASHRAE Guideline 14. 2014. "ASHRAE Guideline 14-2014: Measurement of Energy, Demand, and Water Savings."

Azmi, Nabeeha Amatullah, Azhaili Baharun, Müslüm Arıcı, and Siti Halipah Ibrahim. 2023. "Improving Thermal Comfort in Mosques of Hot-Humid Climates through Passive and Low-Energy Design Strategies." *Frontiers of Architectural Research* 12 (2): 361–85. https://doi.org/10.1016/j.foar.2022.07.001.

Baba, Fuad Mutasim, Muhannad Haj Hussein, Suha Saleh, Mutasim Baba, and Jihad Awad. 2023. "Mitigating Undercooling and Overheating Risk in Existing Desert Schools under Current and Future Climate Using Validated Building Simulation Model." *Building and Environment* 245 (November):110871. https://doi.org/10.1016/J.BUILDENV.2023.110871.

Balocco, Carla. 2007. "Daily Natural Heat Convection in a Historical Hall." *Journal of Cultural Heritage* 8 (4): 370–76. https://doi.org/10.1016/j.culher.2007.04.004.

Balocco, Carla, and Giuseppe Grazzini. 2007. “Plant Refurbishment in Historical Buildings Turned into Museum.” *Energy and Buildings* 39 (6): 693–701. https://doi.org/10.1016/j.enbuild.2006.06.012.

———. 2009. “Numerical Simulation of Ancient Natural Ventilation Systems of Historical Buildings. A Case Study in Palermo.” *Journal of Cultural Heritage* 10 (2): 313–18. https://doi.org/10.1016/j.culher.2008.03.008.

Bamdad, Keivan, Soha Matour, Nima Izadyar, and Tim Law. 2022. “Introducing Extended Natural Ventilation Index for Buildings under the Present and Future Changing Climates.” *Building and Environment* 226 (December):109688. https://doi.org/10.1016/j.buildenv.2022.109688.

Bamdad, Keivan, Soha Matour, Nima Izadyar, and Sara Omrani. 2022. “Impact of Climate Change on Energy Saving Potentials of Natural Ventilation and Ceiling Fans in Mixed-Mode Buildings.” *Building and Environment* 209 (February):108662. https://doi.org/10.1016/J.BUILDENV.2021.108662.

Bay, Ezgi, Antonio Martinez-Molina, and William A. Dupont. 2022. “Assessment of Natural Ventilation Strategies in Historical Buildings in a Hot and Humid Climate Using Energy and CFD Simulations.” *Journal of Building Engineering* 51 (July). https://doi.org/10.1016/j.jobe.2022.104287.

Belcher, S. E., J. N. Hacker, and D. S. Powell. 2005. “Constructing Design Weather Data for Future Climates.” *Http://Dx.Doi.Org/10.1191/0143624405bt112oa* 26 (1): 49–61. https://doi.org/10.1191/0143624405BT112OA.

Bienvenido-Huertas, David, Miguel León-Muñoz, Juan Jesús Martín-del-Río, and Carlos Rubio-Bellido. 2021. “Analysis of Climate Change Impact on the Preservation of Heritage Elements

in Historic Buildings with a Deficient Indoor Microclimate in Warm Regions." *Building and Environment* 200 (August):107959. https://doi.org/10.1016/J.BUILDENV.2021.107959.

Campagna, Ludovica Maria, and Francesco Fiorito. 2022. "On the Impact of Climate Change on Building Energy Consumptions: A Meta-Analysis." *Energies 2022, Vol. 15, Page 354* 15 (1): 354. https://doi.org/10.3390/EN15010354.

"CFD: MicroFlo User Guide IES VE 2015." n.d.

Chassagne, Pierre, Elias Bou-Saïd, Ario Ceccotti, Jean-François Jullien, and Marco Togni. 2007. "The Contribution of Numerical Simulation for the Diagnosis of the Conservation of Art Objects: Application to Antonio Santucci's Armillary Sphere of the 16th Century." *Journal of Cultural Heritage* 8 (3): 215–22. https://doi.org/10.1016/j.culher.2007.04.001.

Chen, Yujiao, Zheming Tong, and Ali Malkawi. 2017. "Investigating Natural Ventilation Potentials across the Globe: Regional and Climatic Variations." *Building and Environment* 122 (September):386–96. https://doi.org/10.1016/j.buildenv.2017.06.026.

Cho, Hyun Mi, Beom Yeol Yun, Young Uk Kim, Hyeonseong Yuk, and Sumin Kim. 2022a. "Integrated Retrofit Solutions for Improving the Energy Performance of Historic Buildings through Energy Technology Suitability Analyses: Retrofit Plan of Wooden Truss and Masonry Composite Structure in Korea in the 1920s." *Renewable and Sustainable Energy Reviews* 168 (October). https://doi.org/10.1016/j.rser.2022.112800.

———. 2022b. "Integrated Retrofit Solutions for Improving the Energy Performance of Historic Buildings through Energy Technology Suitability Analyses: Retrofit Plan of Wooden Truss and Masonry Composite Structure in Korea in the 1920s." *Renewable and Sustainable Energy Reviews* 168 (October):112800. https://doi.org/10.1016/J.RSER.2022.112800.

Cirrincione, Laura, Antonino Marvuglia, and Gianluca Scaccianoce. 2021. "Assessing the Effectiveness of Green Roofs in Enhancing the Energy and Indoor Comfort Resilience of Urban Buildings to Climate Change: Methodology Proposal and Application." *Building and Environment* 205 (November):108198. https://doi.org/10.1016/J.BUILDENV.2021.108198.

Clayton, Susan. 2021. "Climate Change and Mental Health." *Current Environmental Health Reports* 8 (1): 1–6. https://doi.org/10.1007/s40572-020-00303-3.

"Climate.Onebuilding.Org." n.d. Accessed April 23, 2024. https://climate.onebuilding.org/.

Coelho, Guilherme B.A., and Fernando M.A. Henriques. 2021. "Performance of Passive Retrofit Measures for Historic Buildings That House Artefacts Viable for Future Conditions." *Sustainable Cities and Society* 71 (August). https://doi.org/10.1016/j.scs.2021.102982.

Corgnati, Stefano Paolo, and Marco Perino. 2013. "CFD Application to Optimise the Ventilation Strategy of Senate Room at Palazzo Madama in Turin (Italy)." *Journal of Cultural Heritage* 14 (1): 62–69. https://doi.org/10.1016/j.culher.2012.02.007.

Debailleux, Laurent. 2015. "Indexing System for Recognizing Traditional Timber-Framed Structures." *International Journal of Architectural Heritage* 9 (5): 529–41. https://doi.org/10.1080/15583058.2013.824045.

Disclaimers Suggested Citation Production Penrose CDB. 2022. www.globalabc.org.

Dutta, Arindam. 2021. "Energy Conservation and Its Impact on Climate Change." In *Environmental Management: Issues and Concerns in Developing Countries*, 139–50. Cham: Springer International Publishing. https://doi.org/10.1007/978-3-030-62529-0_8.

Emmerich, Steven J, W Stuart Dols, and James W Axley. n.d. "Natural Ventilation Review and Plan for Design and Analysis Tools."

EnergyPlus™. n.d. "EnergyPlus." Accessed November 24, 2023. https://energyplus.net/.

Etheridge, David. 2011. *Natural Ventilation of Buildings: Theory, Measurement and Design*. Wiley.

Everett, Donald E. 1999a. *San Antonio's Monte Vista: Architecture and Society in a Gilded Age, 1890-1930*. San Antonio, TX: Maverick Pub. Co.

———. 1999b. *San Antonio's Monte Vista: Architecture and Society in a Gilded Age, 1890-1930*. San Antonio, TX: Maverick Pub. Co.

Fatnassi, Hicham, Pierre Emmanuel Bournet, Thierry Boulard, Jean Claude Roy, Francisco D. Molina-Aiz, and Rashyd Zaaboul. 2023. "Use of Computational Fluid Dynamic Tools to Model the Coupling of Plant Canopy Activity and Climate in Greenhouses and Closed Plant Growth Systems: A Review." *Biosystems Engineering* 230 (June):388–408. https://doi.org/10.1016/j.biosystemseng.2023.04.016.

Faubel, Carlos, Athanasios Ioannis Arvanitidis, Layla Iskandar, Antonio Martinez-Molina, and Miltiadis Alamaniotis. 2024. "Comparative Analysis of Artificial Intelligence Models for Real-Time and Future Forecasting of Environmental Conditions: A Wood-Frame Historic Building Case Study." *Journal of Building Engineering* 98 (December):111474. https://doi.org/10.1016/J.JOBE.2024.111474.

Faubel, Carlos, Antonio Martinez-Molina, and Jae Yong Suk. 2024. "Calculation of CO2 Generation and Required Fresh Air Rates in a High-Intensity Physical Athletic Facility." *Journal of Building Engineering* 82 (April):108289. https://doi.org/10.1016/J.JOBE.2023.108289.

Fiocchi, L. Carl, Benjamin S. Weil, and Simi Hoque. 2014. "Matching Building Energy Simulation Results against Measured Data with Weather File Compensation Factors." *ASHRAE Conference-Papers* 120:397–404.

Fiorito, Francesco, Giandomenico Vurro, Francesco Carlucci, Ludovica Maria Campagna, Mariella De Fino, Salvatore Carlucci, and Fabio Fatiguso. 2022. "Adaptation of Users to Future Climate Conditions in Naturally Ventilated Historic Buildings: Effects on Indoor Comfort." *Energies* 15 (14). https://doi.org/10.3390/en15144984.

Franzen, Christoph. 2015. "Building Inherent Historic Energy Concept and Energy Management." In *Energy Efficiency Solutions for Historic Buildings*, 67–68.

Fumo, Nelson, Pedro Mago, and Rogelio Luck. 2010. "Methodology to Estimate Building Energy Consumption Using EnergyPlus Benchmark Models." *Energy and Buildings* 42 (12): 2331–37. https://doi.org/10.1016/j.enbuild.2010.07.027.

Ge, Jian, Jiapan Lu, Jindong Wu, Xiaoyu Luo, and Fanghua Shen. 2022. "Suitable and Energy-Saving Retrofit Technology Research in Traditional Wooden Houses in Jiangnan, South China." *Journal of Building Engineering* 45 (January). https://doi.org/10.1016/j.jobe.2021.103550.

Gilani, Sara, and William O'Brien. 2021. "Natural Ventilation Usability under Climate Change in Canada and the United States." *Building Research & Information* 49 (4): 367–86. https://doi.org/10.1080/09613218.2020.1760775.

"HadCM3 Climate Scenario Data." n.d. Accessed June 24, 2024. https://www.ipcc-data.org/sim/gcm_clim/SRES_TAR/hadcm3_download.html.

Hensen, Jan. n.d. "Simulation of Building Energy and Indoor Environmental Quality-Some Weather Data Issues." http://homepages.strath.ac.uk/~clcs31.

Hensley, Jo Ellen, and Antonio Aguilar. 2011. "Preservation Brief 3: Improving the Energy Efficiency in Historic Buildings." Washington DC. http://www.nps.gov/history/hps/tps/briefs/brief03.htm.

Huang, Jianping, Guolong Zhang, Yanting Zhang, Xiaodan Guan, Yun Wei, and Ruixia Guo. 2020. "Global Desertification Vulnerability to Climate Change and Human Activities." *Land Degradation & Development* 31 (11): 1380–91. https://doi.org/10.1002/ldr.3556.

Huddleston, Scott. 2022. "Long-Neglected 1906 Kelso House in Monte Vista Has Beautiful New Exterior — More Work Is Needed." *San Antonio Express News*, 2022. https://www.expressnews.com/news/local/article/1906-Kelso-House-in-Monte-Vista-restoration-work-17017952.php.

Hutkai, K, and D Katunský. 2021. "Insulation of Historic Buildings and Case Study Simulation." *IOP Conference Series: Materials Science and Engineering* 1209 (1): 012003. https://doi.org/10.1088/1757-899X/1209/1/012003.

IES VE. n.d. "IES VE." Accessed April 24, 2024. https://www.iesve.com/.

IESVE. 2021. "IESVE Application User Guides." 2021.

Integrated Environmental Solutions Limited (IES). n.d. "VistaPro User Guide." Accessed November 19, 2023. VistaPro User Guide.

Intergovernmental Panel on Climate Change. n.d. *Climate Change 2014 : Synthesis Report : Longer Report.*

Intergovernmental Panel on Climate Change. Working Group III, and Ottmar Edenhofer. 2014. *Climate Change 2014 : Mitigation of Climate Change : Working Group III Contribution to the Fifth Assessment Report of the Intergovernmental Panel on Climate Change*.

Iskandar, Layla, Ezgi Bay-Sahin, Antonio Martinez-Molina, and Saadet Toker Beeson. 2024. "Evaluation of Passive Cooling through Natural Ventilation Strategies in Historic Residential Buildings Using CFD Simulations." *Energy and Buildings* 308 (April):114005. https://doi.org/10.1016/J.ENBUILD.2024.114005.

Iskandar, Layla, Carlos Faubel, Antonio Martinez-Molina, and Saadet Toker Beeson. 2024. "Quantification of Inherent Energy Efficient Features in Historic Buildings under Hot and Humid Conditions." *Energy and Buildings* 319 (September):114546. https://doi.org/10.1016/J.ENBUILD.2024.114546.

Jentsch, Mark F., Patrick A.B. James, Leonidas Bourikas, and Abu Bakr S. Bahaj. 2013. "Transforming Existing Weather Data for Worldwide Locations to Enable Energy and Building Performance Simulation under Future Climates." *Renewable Energy* 55 (July):514–24. https://doi.org/10.1016/J.RENENE.2012.12.049.

Jiru, Teshome Edae, and Girma Tsegaye Bitsuamlak. 2010. "Application of CFD in Modelling Wind-Induced Natural Ventilation of Buildings - A Review." *International Journal of Ventilation* 9 (2): 131–47. https://doi.org/10.1080/14733315.2010.11683875.

Jogdand, Onkar K. 2020. *Study on the Effect of Global Warming and Greenhouse Gases on Environmental System*. 1st ed. Apple Academic Press.

Karaiskos, Panos, Antonio Martinez-Molina, and Miltiadis Alamaniotis. 2023. "Analyzing Indoor Air Pollutants in Naturally Ventilated Athletic Facilities. A Case of Study." *Journal of Building Engineering* 77 (October):107457. https://doi.org/10.1016/J.JOBE.2023.107457.

Kopec, Dak. 2017. *Health and Well-Being for Interior Architecture*. Routledge.

Kottek, Markus, Jürgen Grieser, Christoph Beck, Bruno Rudolf, and Franz Rubel. 2006. "World Map of the Köppen-Geiger Climate Classification Updated." *Meteorologische Zeitschrift* 15 (3): 259–63. https://doi.org/10.1127/0941-2948/2006/0130.

Kumar, Pakhee, Benjamin Wright, and Athina Petsou. 2024. "Overheating in Historic Buildings in the UK: An Exploratory Study of Overheating Risks, Building Performance, and Thermal Comfort." *Heritage* 7 (9): 4829–54. https://doi.org/10.3390/heritage7090229.

Lee, June-Yi, Jochem Marotzke, Govindasamy Bala, Sebastian Milinski, Kyung-Sook Yun, Aurélien Ribes, Alex C Ruane, et al. n.d. “Chapter 4: Future Global Climate: Scenario-Based Projections and Near-Term Information,” 553–672. Accessed December 18, 2024. https://doi.org/10.1017/9781009157896.006.

Lerma, Carlos, Júlia G. Borràs, Ángeles Mas, M. Eugenia Torner, Jose Vercher, and Enrique Gil. 2021. “Evaluation of Hygrothermal Behaviour in Heritage Buildings through Sensors, CFD Modelling and IRT.” *Sensors 2021, Vol. 21, Page 566* 21 (2): 566. https://doi.org/10.3390/S21020566.

Liu, Pei-Chun, Hsien-Te Lin, and Jung-Hua Chou. 2009. “Evaluation of Buoyancy-Driven Ventilation in Atrium Buildings Using Computational Fluid Dynamics and Reduced-Scale Air Model.” *Building and Environment* 44 (9): 1970–79. https://doi.org/10.1016/j.buildenv.2009.01.013.

Liu, Sheng, Yu Ting Kwok, Kevin Ka Lun Lau, Wanlu Ouyang, and Edward Ng. 2020. “Effectiveness of Passive Design Strategies in Responding to Future Climate Change for Residential Buildings in Hot and Humid Hong Kong.” *Energy and Buildings* 228 (December). https://doi.org/10.1016/j.enbuild.2020.110469.

Luo, Zhiwen, Jianing Zhao, Jun Gao, and Lixia He. 2007. “Estimating Natural-Ventilation Potential Considering Both Thermal Comfort and IAQ Issues.” *Building and Environment* 42 (6): 2289–98. https://doi.org/10.1016/j.buildenv.2006.04.024.

Martinez-Molina, Antonio, and Miltiadis Alamaniotis. 2020. “Enhancing Historic Building Performance with the Use of Fuzzy Inference System to Control the Electric Cooling System.” *Sustainability 2020, Vol. 12, Page 5848* 12 (14): 5848. https://doi.org/10.3390/SU12145848.

Martínez-Molina, Antonio, Isabel Tort-Ausina, Soolyeon Cho, and José Luis Vivancos. 2016. "Energy Efficiency and Thermal Comfort in Historic Buildings: A Review." *Renewable and Sustainable Energy Reviews* 61 (August):70–85. https://doi.org/10.1016/J.RSER.2016.03.018.

Martinez-Molina, Antonio, Kelsey Williamson, and William Dupont. 2022. "Thermal Comfort Assessment of Stone Historic Religious Buildings in a Hot and Humid Climate during Cooling Season. A Case Study." *Energy and Buildings* 262 (May):111997. https://doi.org/10.1016/J.ENBUILD.2022.111997.

Masoumi, Hamid Reza, Nasim Nejati, and Amin Alah Ahadi. 2017. "Learning from the Heritage Architecture: Developing Natural Ventilation in Compact Urban Form in Hot-Humid Climate: Case Study of Bushehr, Iran." *International Journal of Architectural Heritage* 11 (3): 415–32. https://doi.org/10.1080/15583058.2016.1238971.

Meteostat. n.d. "San Antonio International Airport Weather Data." Accessed April 17, 2024. https://meteostat.net/en/station/72253?t=2022-05-01/2022-09-30.

Nagasue, Momoka, Haruka Kitagawa, Takashi Asawa, and Tetsu Kubota. 2024. "A Systematic Review of Passive Cooling Methods in Hot and Humid Climates Using a Text Mining-Based Bibliometric Approach." *Sustainability* 16 (4): 1420. https://doi.org/10.3390/su16041420.

"National Renewable Energy Laboratory (NREL) Home Page | NREL." n.d. Accessed April 23, 2024. https://www.nrel.gov/.

National Trust for Historic Preservation. n.d. "Energy Advice for Owners of Historic and Older Homes | US EPA ARCHIVE DOCUMENT." www.PreservationNation.org.

Pajek, Luka, Matic Možina, Pravin Diliban Nadarajah, Manoj Kumar Singh, and Mitja Košir. 2024. "Future-Proofing a Naturally Ventilated Log House: A Case Study of Adaptive

Thermal Comfort under Climate Change Impact." *Energy and Buildings* 307 (March):113951. https://doi.org/10.1016/j.enbuild.2024.113951.

Palermo, Valentina, Claire L. Walsh, Richard J. Dawson, Alberto Fichera, and Giuseppe Inturri. 2018. "Multi-Sector Mitigation Strategies at the Neighbourhood Scale." *Journal of Cleaner Production* 187 (June):893–902. https://doi.org/10.1016/j.jclepro.2018.03.223.

Pérez-Vega, Cuauhtémoc, José Armando Ramírez-Arias, Irineo Lorenzo López-Cruz, Ramón Arteaga-Ramírez, and Rocío Cervantes-Osornio. 2021. "3D Computational Fluid Dynamics Modeling of Temperature and Humidity in a Humidified Greenhouse." *Ingeniería Agrícola y Biosistemas* 13 (1): 17–31. https://doi.org/10.5154/R.INAGBI.2020.10.060.

Philipsborn, Rebecca, and Kevin Chan. 2021. "Child Health in a Changing Climate." In , 213–23. https://doi.org/10.1142/9789811213946_0027.

Pirani, Anna, Jan S. Fuglestvedt, Edward Byers, Brian O'Neill, Keywan Riahi, June-Yi Lee, Jochem Marotzke, Steven K. Rose, Roberto Schaeffer, and Claudia Tebaldi. 2024. "Scenarios in IPCC Assessments: Lessons from AR6 and Opportunities for AR7." *Npj Climate Action 2024 3:1* 3 (1): 1–7. https://doi.org/10.1038/s44168-023-00082-1.

Plaga, Leonie Sara, and Valentin Bertsch. 2023. "Methods for Assessing Climate Uncertainty in Energy System Models — A Systematic Literature Review." *Applied Energy* 331 (February):120384. https://doi.org/10.1016/J.APENERGY.2022.120384.

Posani, Magda, Maria Do Rosario Veiga, and Vasco Peixoto de Freitas. 2021. "Towards Resilience and Sustainability for Historic Buildings: A Review of Envelope Retrofit Possibilities and a Discussion on Hygric Compatibility of Thermal Insulations." *International Journal of Architectural Heritage* 15 (5): 807–23. https://doi.org/10.1080/15583058.2019.1650133.

Power of Preservation Foundation. 2022. “Power of Preservation Foundation.” 2022. https://powerofpreservation.org/kelso-house.

Pracchi, Valeria. 2014. “Historic Buildings and Energy Efficiency.” *The Historic Environment: Policy & Practice* 5 (2): 210–25. https://doi.org/10.1179/1756750514Z.00000000052.

Rajčić, Vlatka, Ana Skender, and Domagoj Damjanović. 2018. “An Innovative Methodology of Assessing the Climate Change Impact on Cultural Heritage.” *International Journal of Architectural Heritage* 12 (1): 21–35. https://doi.org/10.1080/15583058.2017.1354094.

Ramdlan, G.G.G., A. I. Siswantara, D.A. Budiarso, and H. Pujowidodo. 2016. “Turbulence Model and Validation of Air Flow in Wind Tunnel.” *International Journal of Technology* 7 (8): 1362–71.

Rodrigues, Eugénio, Marco S. Fernandes, and David Carvalho. 2023. “Future Weather Generator for Building Performance Research: An Open-Source Morphing Tool and an Application.” *Building and Environment* 233 (April):110104. https://doi.org/10.1016/J.BUILDENV.2023.110104.

Royapoor, Mohammad, and Tony Roskilly. 2015. “Building Model Calibration Using Energy and Environmental Data.” *Energy and Buildings* 94 (May):109–20. https://doi.org/10.1016/j.enbuild.2015.02.050.

Ryan, Emily M., and Thomas F. Sanquist. 2012. “Validation of Building Energy Modeling Tools under Idealized and Realistic Conditions.” *Energy and Buildings* 47 (April):375–82. https://doi.org/10.1016/j.enbuild.2011.12.020.

Savicki, Darci Luiz, Antonio Goulart, and Gabriel Zardo Becker. 2021. “A Simplified K- ϵ Turbulence Model.” *Journal of the Brazilian Society of Mechanical Sciences and Engineering* 43 (8). https://doi.org/10.1007/s40430-021-03084-4.

Sharmina, Maria. 2017. “Low-Carbon Scenarios for Russia’s Energy System: A Participative Backcasting Approach.” *Energy Policy* 104 (May):303–15. https://doi.org/10.1016/j.enpol.2017.02.009.

Sørensen, D.N., and P.V. Nielsen. 2003. “Quality Control of Computational Fluid Dynamics in Indoor Environments.” *Indoor Air*, no. 13, 2–17. www.blackwellpublishing.com/ina.

The Future of Cooling. 2018. OECD. https://doi.org/10.1787/9789264301993-en.

“The Secretary of the Interior’s Standards for the Treatment of Historic Properties - Technical Preservation Services (U.S. National Park Service).” n.d. Accessed June 29, 2024. https://www.nps.gov/orgs/1739/secretary-standards-treatment-historic-properties.htm.

Tiberio, Alberto Jiménez, and Pablo Branchi. 2013. “A Study of Air Leakage in Residential Buildings.” *Conference and Exhibition - 2013 International Conference on New Concepts in Smart Cities: Fostering Public and Private Alliances, SmartMILE 2013*. https://doi.org/10.1109/SMARTMILE.2013.6708180.

Tonn, Bruce, Beth Hawkins, Erin Rose, and Michaela Marincic. 2021. “A Futures Perspective of Health, Climate Change and Poverty in the United States.” *Futures* 131 (August):102759. https://doi.org/10.1016/j.futures.2021.102759.

US Department of Commerce. 2022. “National Weather Service.” 2022. https://www.weather.gov/wrh/Climate?wfo=ewx.

Wang, Bing, and Ali Malkawi. 2019. “Design-Based Natural Ventilation Evaluation in Early Stage for High Performance Buildings.” *Sustainable Cities and Society* 45 (February):25–37. https://doi.org/10.1016/j.scs.2018.11.024.

Webb, Amanda L. 2017. “Energy Retrofits in Historic and Traditional Buildings: A Review of Problems and Methods.” *Renewable and Sustainable Energy Reviews*. Elsevier Ltd. https://doi.org/10.1016/j.rser.2017.01.145.

WMO. n.d. *WMO Statement on the State of the Global Climate in 2021 = State of the Global Climate 2021*.

Xie, Xiaoxiong, Zhiwen Luo, Sue Grimmond, and Ting Sun. 2023. “Impact of Building Density on Natural Ventilation Potential and Cooling Energy Saving across Chinese Climate Zones.” *Building and Environment* 244 (October):110621. https://doi.org/10.1016/j.buildenv.2023.110621.

Yan, Da, Jianjun Xia, Waiyin Tang, Fangting Song, Xiaoliang Zhang, and Yi Jiang. 2008. “DeST — An Integrated Building Simulation Toolkit Part I: Fundamentals.” *Building Simulation* 1 (2): 95–110. https://doi.org/10.1007/s12273-008-8118-8.

Yassaghi, H., Nariman Mostafavi, and Simi Hoque. 2019. “Evaluation of Current and Future Hourly Weather Data Intended for Building Designs: A Philadelphia Case Study.” *Energy and Buildings* 199 (September):491–511. https://doi.org/10.1016/J.ENBUILD.2019.07.016.

Yassaghi, Hamed, Patrick L. Gurian, and Simi Hoque. 2020. “Propagating Downscaled Future Weather File Uncertainties into Building Energy Use.” *Applied Energy* 278 (November):115655. https://doi.org/10.1016/J.APENERGY.2020.115655.

Yin, Wei, Guoqiang Zhang, Wei Yang, and Xiao Wang. 2010. “Natural Ventilation Potential Model Considering Solution Multiplicity, Window Opening Percentage, Air Velocity and Humidity in China.” *Building and Environment* 45 (2): 338–44. https://doi.org/10.1016/j.buildenv.2009.06.012.

Yohana, Eflita, Bambang Yunianto, Ratrya Putra Hunadika, Shofwan Bahar, and Azza Alifa Muhammad. 2017. “CFD Analysis of Temperature Distribution and Relative Humidity in Humidifying Sample House with Liquid Desiccant Concentration of 50% and Temperature of 10 °C.” *Advanced Science Letters* 23 (3): 2243–45. https://doi.org/10.1166/ASL.2017.8719.

Yuk, Hyeonseong, Ho Hyeon Jo, Ji Yong Choi, Jihee Nam, Seong Jin Chang, and Sumin Kim. 2023. “Evaluation of Suitability for Passive Retrofit of Wooden Roof Considering the Specificity of Historic Buildings.” *Building and Environment* 242 (August):110608. https://doi.org/10.1016/j.buildenv.2023.110608.

Zhang, Xuelin, A.U. Weerasuriya, and K.T. Tse. 2020. “CFD Simulation of Natural Ventilation of a Generic Building in Various Incident Wind Directions: Comparison of Turbulence Modelling, Evaluation Methods, and Ventilation Mechanisms.” *Energy and Buildings* 229 (December):110516. https://doi.org/10.1016/j.enbuild.2020.110516.

Step 1: Environmental data collection campaign

Using indoor and outdoor temperature and relative humidity data loggers

Step 2: Modeling the case study building in IES VE

Using actual floor plan and in-situ measurements

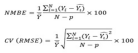

Step 3: Validating the model

Using measured environmental data and ASHRAE indices

Step 4: Generating future weather data in CCWorldWeatherGen

Using the Morphing technique

Step 5: Simulating energy performance of different natural ventilation strategies in the present and future

Analyzing environmental conditions for each natural ventilation strategy in the present, 2050, and 2080

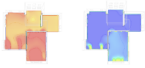

Step 6: CFD simulations for two representative days (spring and summer)

Analyzing temperature and air velocity distributions

Figure 1. Applied methodology.

Figure 2. The Kelso House after the exterior restoration, as viewed from the southeast orientation. Source: Assaad Akle, 2023.

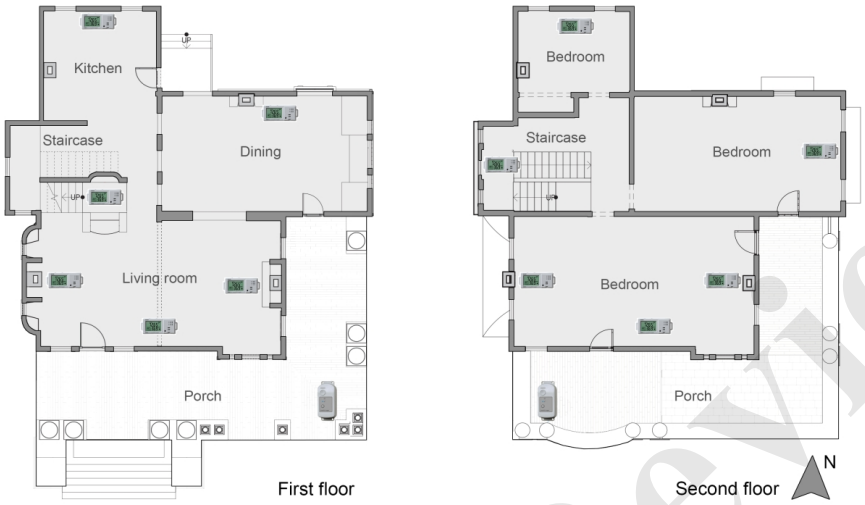

Figure 3. Placement of the indoor and outdoor temperature and relative humidity data loggers on the first and second floors. An additional data logger was placed on the attic level (not shown).

Figure 4. Simplified model of the building simulated in the IES VE software.

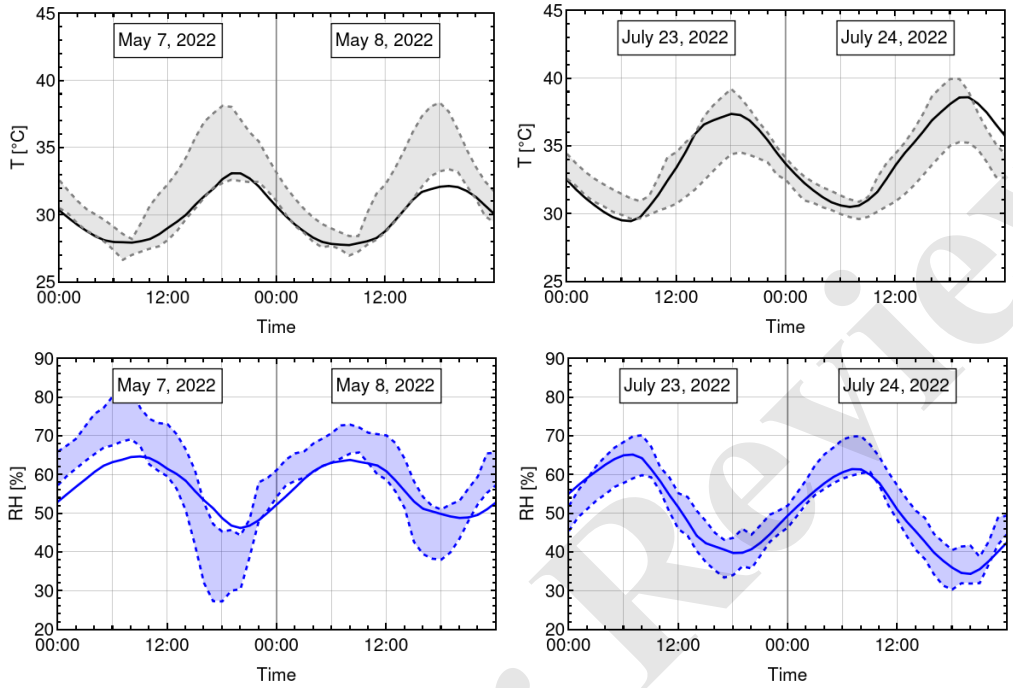

Figure 5. Model validation for the representative days: indoor air temperature (top) and relative humidity (bottom). The solid lines represent simulated values, while the colored bands correspond to the maximum and minimum values recorded over those days.

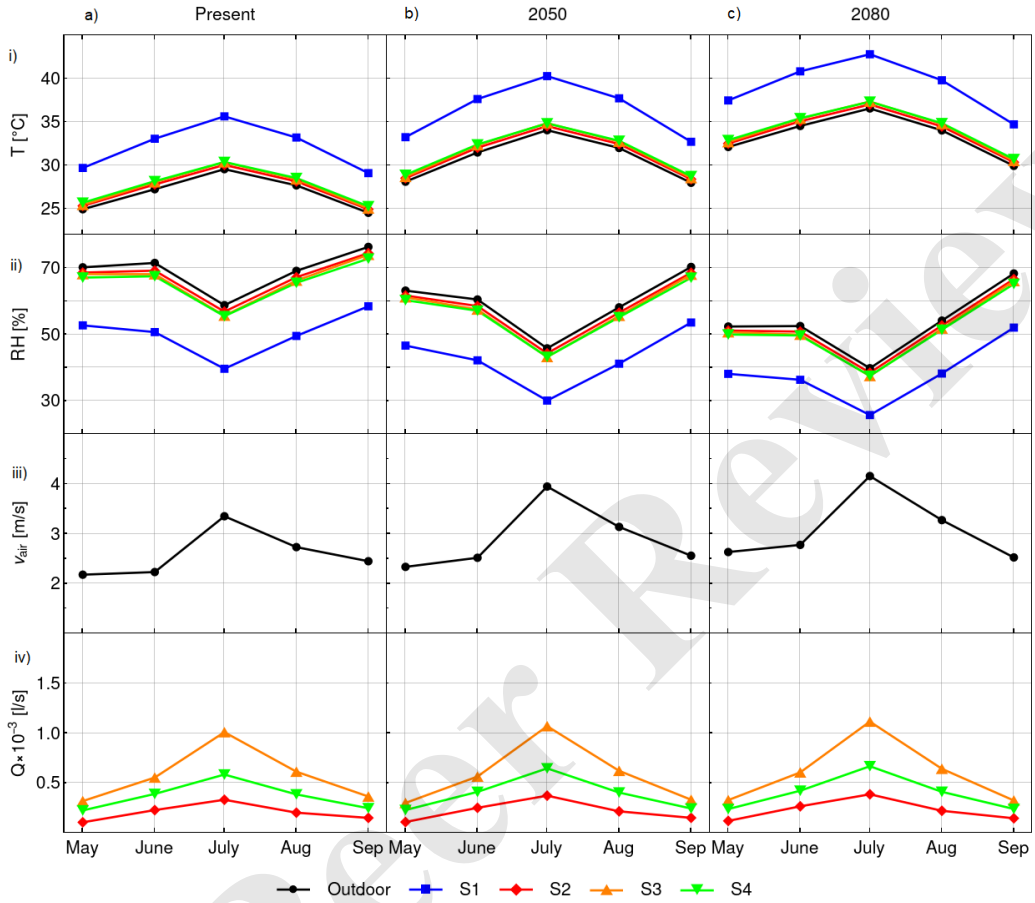

Figure 6. Monthly averages of the environmental variables throughout the cooling season. From top to bottom: i) air temperature and ii) relative humidity, iii) outdoor air velocity, and iv) ventilation rates within the building. From left to right: time evolution of the environmental values for the a) present weather data, b) 2050 weather data, and c) 2080 weather data. Outdoor environmental values correspond to the location of the building in San Antonio, Texas, USA.

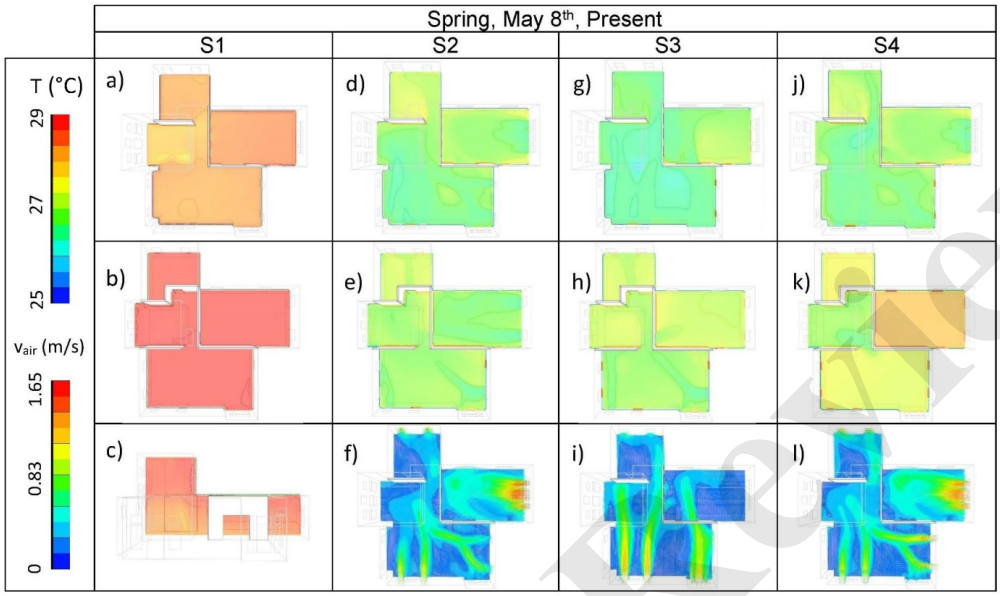

Figure 7. Air temperature and airflow graphs for May 8th using present weather data. From top to bottom row: air temperature (1st floor plan); air temperature (2nd floor plan); air temperature (vertical east-west section through staircase) for S1, and airflow (1st floor plan) for S2, S3, and S4.

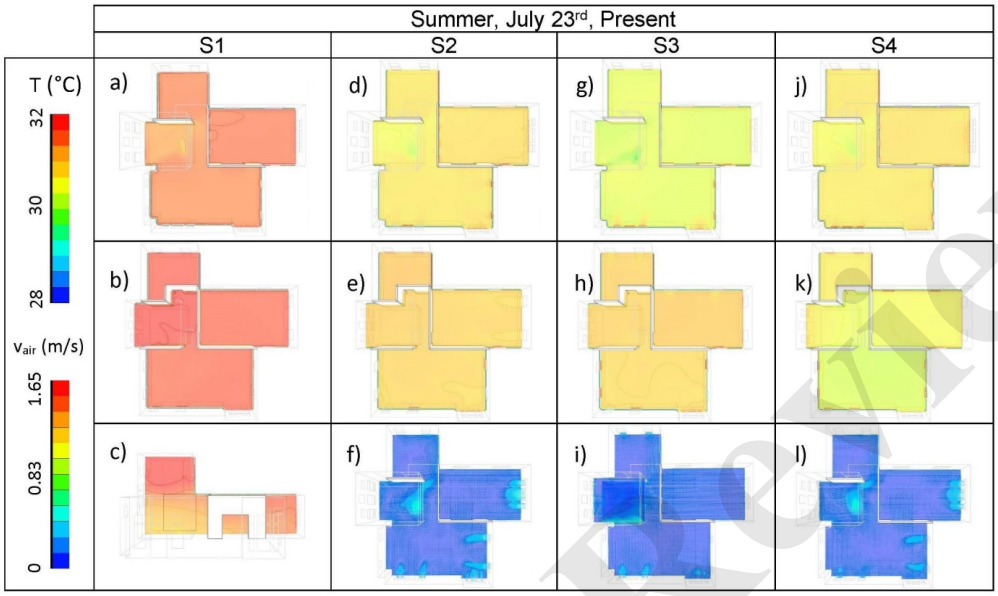

Figure 8. Air temperature and airflow graphs for July 23rd using present weather data. From top to bottom row: air temperature (1st floor plan); air temperature (2nd floor plan); air temperature (vertical east-west section through staircase) for S1, and airflow (1st floor plan) for S2, S3, and S4.

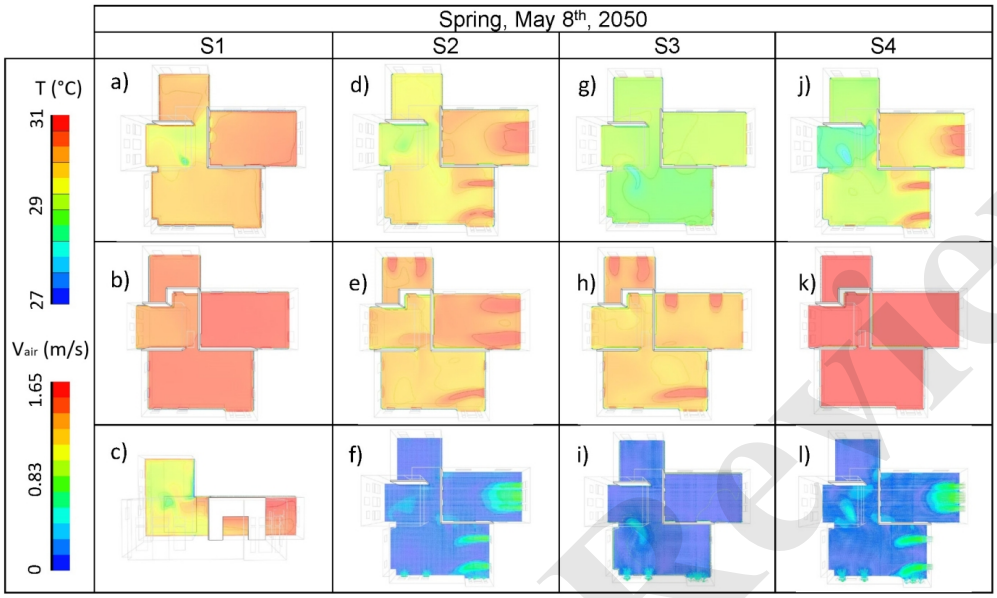

Figure 9. Air temperature and airflow graphs for May 8th, 2050. From top to bottom row: air temperature (1st floor plan); air temperature (2nd floor plan); air temperature (vertical east-west section through staircase) for S1, and airflow (1st floor plan) for S2, S3, and S4.

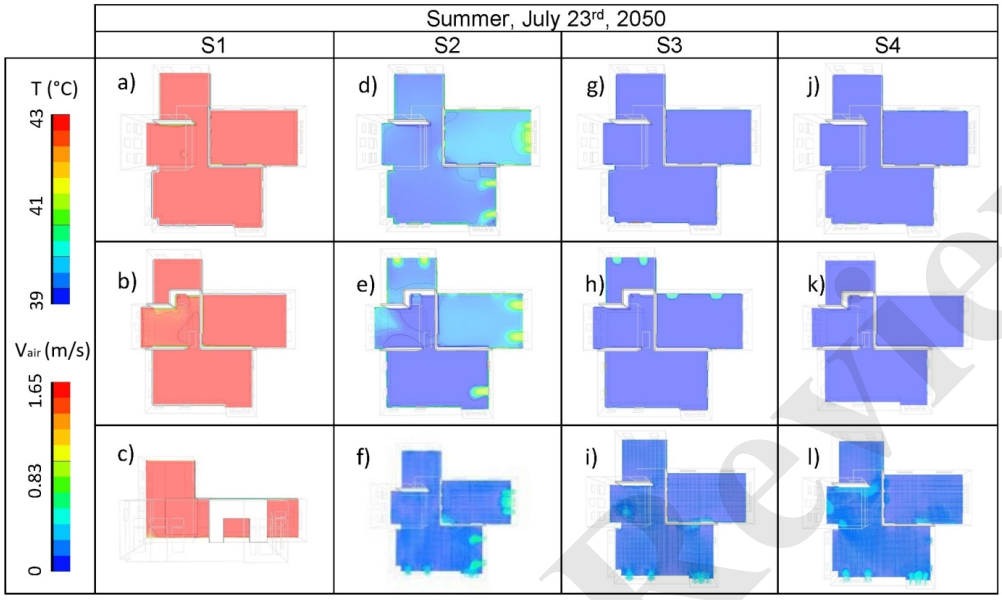

Figure 10. Air temperature and airflow graphs for July 23rd, 2050. From top to bottom row: air temperature (1st floor plan); air temperature (2nd floor plan); air temperature (vertical east-west section through staircase) for S1, and airflow (1st floor plan) for S2, S3, and S4.

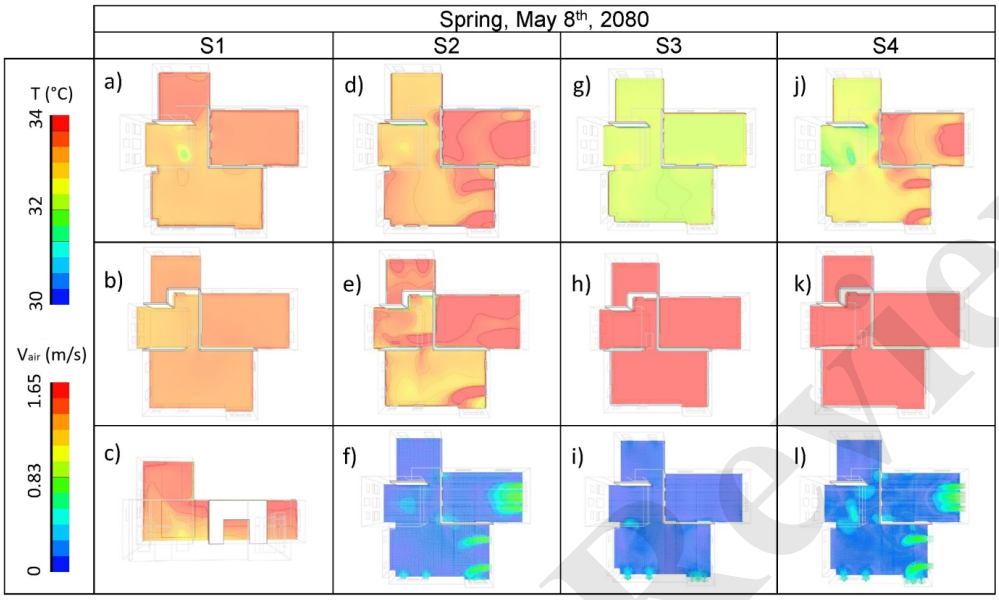

Figure 11. Air temperature and airflow graphs for May 8th, 2080. From top to bottom row: air temperature (1st floor plan); air temperature (2nd floor plan); air temperature (vertical east-west section through staircase) for S1, and airflow (1st floor plan) for S2, S3, and S4.

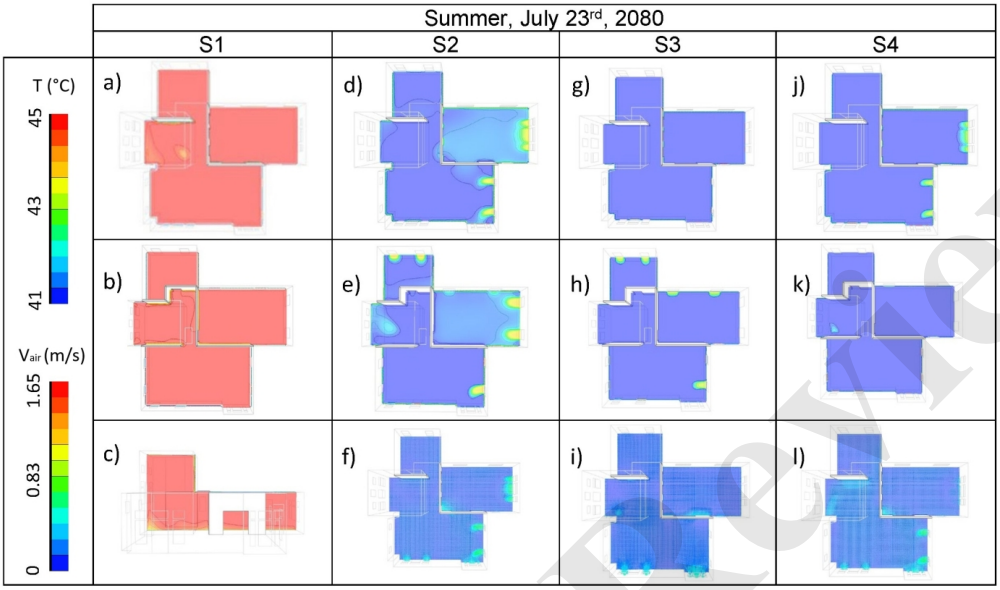

Figure 12. Air temperature and airflow graphs for May 8th, 2080. From top to bottom row: air temperature (1st floor plan); air temperature (2nd floor plan); air temperature (vertical east-west section through staircase) for S1, and airflow (1st floor plan) for S2, S3, and S4.

Table 1. Characteristics of the case study building's envelope.

Characteristic	Description
Exterior walls	Wood-frame walls with wood shingle cladding. U-value = 1.33 W/m^2·K
Roof	Pitched wood-frame roof with wood shingles. U-value = 0.97 W/m^2·K
Floor	Wood joists and hardwood finish. U-value = 2.08 W/m^2·K
Windows	Single-glazed wood windows. U-value = 5.28 W/m^2·K
Infiltration	10 ACH
HVAC system	No HVAC system. Naturally ventilated building.

Table 2. Specifications of the data loggers used in the monitoring campaign.

Environmental conditions	Brand and Model	Range	Accuracy	Response
Indoor Air Temperature	HOBO® MX1101	[-20, 70] °C	0.21 °C	60 sec.
Indoor Relative Humidity	HOBO® MX1101	[1, 90] %	± 2.0 %	20 sec.
Outdoor Air Temperature	HOBO® MX2301A	[-40, 70] °C	0.25 °C	60 sec.
Outdoor Relative Humidity	HOBO® MX2301A	[0, 100] %	± 2.5 %	30 sec.

Table 3. Indoor and outdoor environmental conditions during the cooling period from May to September 2022.

	May	June	July	August	September
Minimum Indoor Air Temperature (°C)	22.4	22.4	29.3	27.4	26.3
Maximum Indoor Air Temperature (°C)	36.9	39.9	41.4	39.3	35.2
Average Indoor Air Temperature (°C)	29.9	33.0	34.3	32.3	30.5
Average Outdoor Air Temperature (°C)	28.3	31.0	32.0	30.5	29.3
Average Indoor Relative Humidity (%)	57.5	49.1	47.9	56.8	58.8
Average Outdoor Relative Humidity (%)	65.5	58.5	57.9	64.5	64.1
Average Outdoor Wind speed (km/h)	19.3	16.5	16.9	13.6	10.0
Average Outdoor Wind direction (degrees)	151	137	151	140	147

Table 4. Natural ventilation strategies analyzed in this study.

Natural ventilation strategy	Description	Openings operation
S1	No natural ventilation	All openings closed
S2	Full natural ventilation	All windows open at full capacity
S3	Cross ventilation	1st and 2nd floor windows open at full capacity on the north and south facades; attic door and windows closed
S4	Stack ventilation	1st floor windows and attic door and windows open; 2nd floor windows closed

Table 5. Model specifications and the building components.

IESVE ModelIT		IESVE Apache			
		Building components	Material	Thickness (mm)	Conductivity (m²K/W)
Volume (m³)	1369.92	Walls	Wood	127	0.46
Ext wall area (m²)	456.33	Partitions	Wood	127	0.47
Openings area (m²)	61.86	Roof	Wood	128	0.91
Floor area (m²)	703.14	Ground floor	Wood	38	0.31
Volume (m³)	1369.92	Windows	Single pane	3	0.15

Table 6. CFD model settings.

IESVE MicroFlo	
Number of cells (million)	3.2-3.4
Max cell aspect ratio	<12:1
Turbulence model	k-e
Grid line merge tolerance (m)	0.01

Table 7. Results of the model validation.

ASHRAE index	ASHRAE 14 accepted range	Environmental variable	May 7th	May 8th	July 23rd	July 24th
NMBE (%)	<±10	Indoor Air temperature	4.32	5.02	-0.28	-2.2
		Indoor Air relative humidity	3.87	4.38	-2.33	2.96
CV(RMSE) (%)	< 30	Indoor Air temperature	5.42	6.23	3.02	3.19
		Indoor Air relative humidity	13.91	8.5	5.84	4.42

Table 8. Average indoor and outdoor (OUT) air temperature (T), and indoor ventilation rates (Q), at 12:00 for the representative days considered in the CFD analysis.

	Spring, May 8th						Summer, July 23rd					
	Present		2050		2080		Present		2050		2080	
	T (°C)	Q (l/s)	T (°C)	Q (l/s)	T (°C)	Q (l/s)	T (°C)	Q (l/s)	T (°C)	Q (l/s)	T (°C)	Q (l/s)
OUT	27.0	-	30.3	-	34.8	-	34.0	-	38.8	-	41.6	-
S1	28.8	-	30.2	-	33.8	-	33.2	-	43.0	-	45.5	-
S2	26.4	130.9	28.7	120.3	32.9	124.4	30.2	127.3	39.3	115.5	42.0	113.8
S3	25.6	1633.8	28.4	218.7	32.4	222.4	29.1	349.9	39.2	264.1	41.9	252.3
S4	25.7	233.7	27.9	215.1	31.7	222.9	29.7	176.1	39.3	152.0	41.9	144.7

Table 9. Monthly average values of the simulated indoor air temperature (T), relative humidity (RH), and ventilation rates (Q) during the cooling seasons. OUT stands for the environmental variables corresponding to the location of the case study building, namely San Antonio, Texas, USA.

		May			Jun			Jul			Aug			Sep		
		T (°C)	RH (%)	Q (l/s)	T (°C)	RH (%)	Q (l/s)	T (°C)	RH (%)	Q (l/s)	T (°C)	RH (%)	Q (l/s)	T (°C)	RH (%)	Q (l/s)
Present	OUT	24.9	70.2	-	27.2	71.5	-	29.6	58.8	-	27.7	69.1	-	24.5	76.3	-
	S1	29.7	52.7	-	33.1	50.7	-	35.7	39.7	-	33.2	49.5	-	29.1	58.5	-
	S2	25.3	68.6	105	27.8	69.2	228	30.0	56.9	332	28.1	67.2	202	24.9	74.4	150
	S3	25.4	68.1	318	28.1	68.1	554	30.4	55.6	1010	28.4	66.2	613	25.0	74.0	364
	S4	25.7	67.1	225	28.2	67.5	390	30.4	55.5	584	28.5	65.5	385	25.3	72.8	247
2050	OUT	28.1	63.2	-	31.5	60.5	-	34.1	45.8	-	32.0	58.1	-	28.0	70.3	-
	S1	33.3	46.6	-	37.7	42.2	-	40.3	30.1	-	37.7	41.2	-	32.7	53.6	-
	S2	28.5	61.7	108	32.0	58.5	251	34.5	44.3	372	32.5	56.5	215	28.4	68.6	150
	S3	28.7	61.2	300	32.3	57.5	564	34.9	43.2	1070	32.7	55.6	622	28.5	68.0	332
	S4	28.9	60.3	228	32.4	57.1	410	34.8	43.2	646	32.8	55.2	404	28.8	67.0	244
2080	OUT	32.1	52.4	-	34.5	52.5	-	36.6	39.8	-	34.0	54.1	-	29.9	68.3	-
	S1	37.5	38.1	-	40.8	36.3	-	42.8	25.7	-	39.8	38.2	-	34.7	52.0	-
	S2	32.5	51.1	119	35.1	50.8	266	37.0	38.5	386	34.5	52.7	221	30.4	66.6	146
	S3	32.7	50.6	328	35.4	49.9	606	37.4	37.5	1116	34.8	51.8	642	30.5	66.1	324
	S4	32.9	50.0	238	35.4	49.7	422	37.3	37.5	668	34.9	51.4	411	30.7	65.2	239